protein homolog containing leucine zipper and tetratricopeptide repeat motifs. *Gene* 1995; **160**: 297–302.
44. Edlich F, Weiwad M, Erdmann F, *et al.* Bcl-2 regulator FKBP38 is activated by Ca2+/calmodulin. *EMBO J* 2005; **24**: 2688–2699.
45. Edlich F, Weiwad M, Wildemann D, *et al.* The specific FKBP38 inhibitor N-(N',N'-dimethylcarboxamidomethyl)cycloheximide has potent neuroprotective and neurotrophic properties in brain ischemia. *J Biol Chem* 2006; **281**: 14961–14970.
46. Nielsen JV, Mitchelmore C, Pedersen KM, Kjaerulff KM, Finsen B, Jensen NA. Fkbp8: novel isoforms, genomic organization, and characterization of a forebrain promoter in transgenic mice. *Genomics* 2004; **83**: 181–192.
47. Bulgakov OV, Eggenschwiler JT, Hong DH, Anderson KV, Li T. FKBP8 is a negative regulator of mouse sonic hedgehog signaling in neural tissues. *Development* 2004; **131**: 2149–2159.
48. Echelard Y, Epstein DJ, St-Jacques B, *et al.* Sonic hedgehog, a member of a family of putative signaling molecules, is implicated in the regulation of CNS polarity. *Cell* 1993; **75**: 1417–1430.
49. Chang DT, Lopez A, von Kessler DP, *et al.* Products, genetic linkage and limb patterning activity of a murine hedgehog gene. *Development* 1994; **120**: 3339–3353.
50. Briscoe J, Ericson J. Specification of neuronal fates in the ventral neural tube. *Curr Opin Neurobiol* 2001; **11**: 43–49.
51. Chiang C, Litingtung Y, Lee E, *et al.* Cyclopia and defective axial patterning in mice lacking Sonic hedgehog gene function. *Nature* 1996; **383**: 407–413.
52. Chen Y, Struhl G. Dual roles for patched in sequestering and transducing Hedgehog. *Cell* 1996; **87**: 553–563.
53. Marigo V, Davey RA, Zuo Y, Cunningham JM, Tabin CJ. Biochemical evidence that patched is the Hedgehog receptor. *Nature* 1996; **384**: 176–179.
54. Price MA, Kalderon D. Proteolysis of cubitus interruptus in Drosophila requires phosphorylation by protein kinase A. *Development* 1999; **126**: 4331–4339.
55. Ohlmeyer JT, Kalderon D. Hedgehog stimulates maturation of Cubitus interruptus into a labile transcriptional activator. *Nature* 1998; **396**: 749–753.
56. Wijgerde M, McMahon JA, Rule M, McMahon AP. A direct requirement for Hedgehog signaling for normal specification of all ventral progenitor domains in the presumptive mammalian spinal cord. *Genes Dev* 2002; **16**: 2849–2864.
57. Goodrich LV, Milenkovic L, Higgins KM, Scott MP. Altered neural cell fates and medulloblastoma in mouse patched mutants. *Science* 1997; **277**: 1109–1113.
58. Shirane M, Nakayama KI. Inherent calcineurin inhibitor FKBP38 targets Bcl-2 to mitochondria and inhibits apoptosis. *Nat Cell Biol* 2003; **5**: 28–37.
59. Waxman L, Whitney M, Pollok BA, Kuo LC, Darke PL. Host cell factor requirement for hepatitis C virus enzyme maturation. *Proc Natl Acad Sci USA* 2001; **98**: 13931–13935.
60. Naito T, Momose F, Kawaguchi A, Nagata K. Involvement of Hsp90 in assembly and nuclear import of influenza virus RNA polymerase subunits. *J Virol* 2007; **81**: 1339–1349.
61. Momose F, Naito T, Yano K, Sugimoto S, Morikawa Y, Nagata K. Identification of Hsp90 as a stimulatory host factor involved in influenza virus RNA synthesis. *J Biol Chem* 2002; **277**: 45306–45314.
62. Burch AD, Weller SK. Herpes simplex virus type 1 DNA polymerase requires the mammalian chaperone hsp90 for proper localization to the nucleus. *J Virol* 2005; **79**: 10740–10749.
63. Kampmueller KM, Miller DJ. The cellular chaperone heat shock protein 90 facilitates Flock House virus RNA replication in Drosophila cells. *J Virol* 2005; **79**: 6827–6837.
64. Connor JH, McKenzie MO, Parks GD, Lyles DS. Antiviral activity and RNA polymerase degradation following Hsp90 inhibition in a range of negative strand viruses. *Virology* 2007; **362**: 109–117.
65. Hu J, Toft DO, Seeger C. Hepadnavirus assembly and reverse transcription require a multi-component chaperone complex which is incorporated into nucleocapsids. *EMBO J* 1997; **16**: 59–68.
66. Hu J, Seeger C. Hsp90 is required for the activity of a hepatitis B virus reverse transcriptase. *Proc Natl Acad Sci USA* 1996; **93**: 1060–1064.
67. Geller R, Vignuzzi M, Andino R, Frydman J. Evolutionary constraints on chaperone-mediated folding provide an antiviral approach refractory to development of drug resistance. *Genes Dev* 2007; **21**: 195–205.
68. Skehel PA, Martin KC, Kandel ER, Bartsch D. A VAMP-binding protein from Aplysia required for neurotransmitter release. *Science* 1995; **269**: 1580–1583.
69. Nishimura Y, Hayashi M, Inada H, Tanaka T. Molecular cloning and characterization of mammalian homologues of vesicle-associated membrane protein-associated (VAMP-associated) proteins. *Biochem Biophys Res Commun* 1999; **254**: 21–26.
70. Skehel PA, Fabian-Fine R, Kandel ER. Mouse VAP33 is associated with the endoplasmic reticulum and microtubules. *Proc Natl Acad Sci USA* 2000; **97**: 1101–1106.
71. Soussan L, Burakov D, Daniels MP, *et al.* ERG30, a VAP-33-related protein, functions in protein trans-

port mediated by COPI vesicles. *J Cell Biol* 1999; **146**: 301–311.
72. Kagiwada S, Hosaka K, Murata M, Nikawa J, Takatsuki A. The Saccharomyces cerevisiae SCS2 gene product, a homolog of a synaptobrevin-associated protein, is an integral membrane protein of the endoplasmic reticulum and is required for inositol metabolism. *J Bacteriol* 1998; **180**: 1700–1708.
73. Weir ML, Klip A, Trimble WS. Identification of a human homologue of the vesicle-associated membrane protein (VAMP)-associated protein of 33 kDa (VAP-33): a broadly expressed protein that binds to VAMP. *Biochem J* 1998; **333**(Pt 2): 247–251.
74. Nelson GA, Ward S. Amoeboid motility and actin in Ascaris lumbricoides sperm. *Exp Cell Res* 1981; **131**: 149–160.
75. Italiano JE Jr, Stewart M, Roberts TM. How the assembly dynamics of the nematode major sperm protein generate amoeboid cell motility. *Int Rev Cytol* 2001; **202**: 1–34.
76. Roberts TM, Stewart M. Acting like actin. The dynamics of the nematode major sperm protein (msp) cytoskeleton indicate a push-pull mechanism for amoeboid cell motility. *J Cell Biol* 2000; **149**: 7–12.
77. Tarr DE, Scott AL. MSP domain proteins. *Trends Parasitol* 2005; **21**: 224–231.
78. Loewen CJ, Roy A, Levine TP. A conserved ER targeting motif in three families of lipid binding proteins and in Opi1p binds VAP. *EMBO J* 2003; **22**: 2025–2035.
79. Pennetta G, Hiesinger PR, Fabian-Fine R, Meinertzhagen IA, Bellen HJ. Drosophila VAP-33A directs bouton formation at neuromuscular junctions in a dosage-dependent manner. *Neuron* 2002; **35**: 291–306.
80. Weir ML, Xie H, Klip A, Trimble WS. VAP-A binds promiscuously to both v- and tSNAREs. *Biochem Biophys Res Commun* 2001; **286**: 616–621.
81. Kaiser SE, Brickner JH, Reilein AR, Fenn TD, Walter P, Brunger AT. Structural basis of FFAT motif-mediated ER targeting. *Structure* 2005; **13**: 1035–1045.
82. Brickner JH, Walter P. Gene recruitment of the activated INO1 locus to the nuclear membrane. *PLoS Biol* 2004; **2**: e342.
83. Funakoshi T, Yasuda S, Fukasawa M, Nishijima M, Hanada K. Reconstitution of ATP- and cytosol-dependent transport of de novo synthesized ceramide to the site of sphingomyelin synthesis in semi-intact cells. *J Biol Chem* 2000; **275**: 29938–29945.
84. Fukasawa M, Nishijima M, Hanada K. Genetic evidence for ATP-dependent endoplasmic reticulum-to-Golgi apparatus trafficking of ceramide for sphingomyelin synthesis in Chinese hamster ovary cells. *J Cell Biol* 1999; **144**: 673–685.
85. Kawano M, Kumagai K, Nishijima M, Hanada K. Efficient trafficking of ceramide from the endoplasmic reticulum to the Golgi apparatus requires a VAMP-associated protein-interacting FFAT motif of CERT. *J Biol Chem* 2006; **281**: 30279–30288.
86. Quintavalle M, Sambucini S, Summa E, *et al*. Hepatitis C virus NS5A is a direct substrate of CKI-alpha, a cellular kinase identified by inhibitor affinity chromatography using specific NS5A hyperphosphorylation inhibitors. *J Biol Chem* 2007; **282**: 5536–5544.
87. Neddermann P, Quintavalle M, Di Pietro C, *et al*. Reduction of hepatitis C virus NS5A hyperphosphorylation by selective inhibition of cellular kinases activates viral RNA replication in cell culture. *J Virol* 2004; **78**: 13306–13314.
88. Burckstummer T, Kriegs M, Lupberger J, Pauli EK, Schmittel S, Hildt E. Raf-1 kinase associates with Hepatitis C virus NS5A and regulates viral replication. *FEBS Lett* 2006; **580**: 575–580.
89. Gao L, Aizaki H, He JW, Lai MM. Interactions between viral nonstructural proteins and host protein hVAP-33 mediate the formation of hepatitis C virus RNA replication complex on lipid raft. *J Virol* 2004; **78**: 3480–3488.
90. Shi ST, Lee KJ, Aizaki H, Hwang SB, Lai MM. Hepatitis C virus RNA replication occurs on a detergent-resistant membrane that cofractionates with caveolin-2. *J Virol* 2003; **77**: 4160–4168.
91. Zhang J, Yamada O, Sakamoto T, *et al*. Down-regulation of viral replication by adenoviral-mediated expression of siRNA against cellular cofactors for hepatitis C virus. *Virology* 2004; **320**: 135–143.
92. Amarilio R, Ramachandran S, Sabanay H, Lev S. Differential regulation of endoplasmic reticulum structure through VAP-Nir protein interaction. *J Biol Chem* 2005; **280**: 5934–5944.
93. Giese SI, Woerz I, Homann S, Tibroni N, Geyer M, Fackler OT. Specific and distinct determinants mediate membrane binding and lipid raft incorporation of HIV-1(SF2) Nef. *Virology* 2006; **355**: 175–191.
94. Brugger B, Glass B, Haberkant P, Leibrecht I, Wieland FT, Krausslich HG. The HIV lipidome: a raft with an unusual composition. *Proc Natl Acad Sci USA* 2006; **103**: 2641–2646.
95. Mannova P, Fang R, Wang H, *et al*. Modification of host lipid raft proteome upon hepatitis C virus replication. *Mol Cell Proteomics* 2006; **5**: 2319–2325.
96. Oomens AG, Bevis KP, Wertz GW. The cytoplasmic tail of the human respiratory syncytial virus F protein plays critical roles in cellular localization of the F protein and infectious progeny production. *J Virol* 2006; **80**: 10465–10477.
97. Chen BJ, Takeda M, Lamb RA. Influenza virus hemagglutinin (H3 subtype) requires palmitoylation of its cytoplasmic tail for assembly: M1 pro-

teins of two subtypes differ in their ability to support assembly. *J Virol* 2005; **79**: 13673–13684.
98. Kapadia SB, Chisari FV. Hepatitis C virus RNA replication is regulated by host geranylgeranylation and fatty acids. *Proc Natl Acad Sci USA* 2005; **102**: 2561–2566.
99. Horton JD, Goldstein JL, Brown MS. SREBPs: activators of the complete program of cholesterol and fatty acid synthesis in the liver. *J Clin Invest* 2002; **109**: 1125–1131.
100. Barba G, Harper F, Harada T, *et al.* Hepatitis C virus core protein shows a cytoplasmic localization and associates to cellular lipid storage droplets. *Proc Natl Acad Sci USA* 1997; **94**: 1200–1205.
101. Moriishi K, Mochizuki R, Moriya K, *et al.* Critical role of PA28gamma in hepatitis C virus-associated steatogenesis and hepatocarcinogenesis. *Proc Natl Acad Sci USA* 2007; **104**: 1661–1666.
102. Aizaki H, Lee KJ, Sung VM, Ishiko H, Lai MM. Characterization of the hepatitis C virus RNA replication complex associated with lipid rafts. *Virology* 2004; **324**: 450–461.
103. Ye J, Wang C, Sumpter R Jr, Brown MS, Goldstein JL, Gale M Jr. Disruption of hepatitis C virus RNA replication through inhibition of host protein geranylgeranylation. *Proc Natl Acad Sci USA* 2003; **100**: 15865–15870.
104. Wang C, Gale M Jr, Keller BC, *et al.* Identification of FBL2 as a geranylgeranylated cellular protein required for hepatitis C virus RNA replication. *Mol Cell* 2005; **18**: 425–434.
105. Ilyin GP, Rialland M, Glaise D, Guguen-Guillouzo C. Identification of a novel Skp2-like mammalian protein containing F-box and leucine-rich repeats. *FEBS Lett* 1999; **459**: 75–79.
106. Shimakami T, Honda M, Kusakawa T, *et al.* Effect of hepatitis C virus (HCV) NS5B-nucleolin interaction on HCV replication with HCV subgenomic replicon. *J Virol* 2006; **80**: 3332–3340.
107. Goh PY, Tan YJ, Lim SP, *et al.* Cellular RNA helicase p68 relocalization and interaction with the hepatitis C virus (HCV) NS5B protein and the potential role of p68 in HCV RNA replication. *J Virol* 2004; **78**: 5288–5298.
108. Machida K, Cheng KT, Lai CK, Jeng KS, Sung VM, Lai MM. Hepatitis C virus triggers mitochondrial permeability transition with production of reactive oxygen species, leading to DNA damage and STAT3 activation. *J Virol* 2006; **80**: 7199–7207.
109. Kawamura H, Govindarajan S, Aswad F, *et al.* HCV core expression in hepatocytes protects against autoimmune liver injury and promotes liver regeneration in mice. *Hepatology* 2006; **44**: 936–944.
110. Yoshida T, Hanada T, Tokuhisa T, *et al.* Activation of STAT3 by the hepatitis C virus core protein leads to cellular transformation. *J Exp Med* 2002; **196**: 641–653.
111. Ogata H, Kobayashi T, Chinen T, *et al.* Deletion of the SOCS3 gene in liver parenchymal cells promotes hepatitis-induced hepatocarcinogenesis. *Gastroenterology* 2006; **131**: 179–193.
112. Moriya K, Fujie H, Shintani Y, *et al.* The core protein of hepatitis C virus induces hepatocellular carcinoma in transgenic mice. *Nat Med* 1998; **4**: 1065–1067.
113. Lerat H, Honda M, Beard MR, *et al.* Steatosis and liver cancer in transgenic mice expressing the structural and nonstructural proteins of hepatitis C virus. *Gastroenterology* 2002; **122**: 352–365.
114. Koike K, Moriya K, Ishibashi K, *et al.* Sialadenitis histologically resembling Sjogren syndrome in mice transgenic for hepatitis C virus envelope genes. *Proc Natl Acad Sci USA* 1997; **94**: 233–236.

JOURNAL OF VIROLOGY, Aug. 2007, p. 8373
0022-538X/07/$08.00+0 doi:10.1128/JVI.01325-07

Vol. 81, No. 16

SPOTLIGHT

Articles of Significant Interest Selected from This Issue by the Editors

Novel Processing of Japanese Encephalitis Virus Capsid Protein

The Japanese encephalitis virus (JEV) capsid protein is generated from a precursor polyprotein by processing with host and viral proteases. Mori et al. (p. 8477–8487) show that further processing of the capsid protein by cathepsin L is involved in the replication of JEV in neural and macrophage cell lines. This work suggests that JEV uses a novel mechanism to infect host cells via cathepsin-mediated processing of the capsid protein.

Nodavirus RNA Polymerase Synthesis Requires Cellular Chaperones

Genome translation is an essential early step in the life cycle of positive-sense RNA viruses and often involves manipulation of the cellular translation apparatus to benefit the invading virus. Castorena et al. (p. 8412–8420) demonstrate that heat shock protein 90, an abundant cellular chaperone implicated in the replication of numerous viruses, facilitates the efficient synthesis of Flock House virus RNA polymerase. This work highlights the diverse mechanisms whereby viruses exploit cellular machinery to accomplish specific tasks to achieve their replication.

Rotavirus-Induced Alteration of Occludin Expression

Rotavirus can affect the intestinal barrier by diminishing the integrity of tight junctions (TJs). Beau et al. (p. 8579–8586) demonstrate that rhesus monkey rotavirus (RRV) alters the expression of occludin, an integral TJ protein, in enterocyte-like Caco-2 cells. The disappearance of occludin from the TJ plane, decrease in the nonphosphorylated form of occludin, and diminished levels of occludin mRNA are antagonized by inhibitors of protein kinase A (PKA). This work suggests that rotavirus uses PKA-dependent mechanisms to alter TJ function, which might in turn contribute to its pathogenicity or dissemination.

Human Immunodeficiency Virus Escape from Potent Neutralizing Antibodies

A recent clinical trial evaluated neutralizing monoclonal antibodies (MAbs) 2F5 and 4E10 targeting the membrane-proximal external region (MPER) of human immunodeficiency virus (HIV) gp41 together with the carbohydrate-specific MAb 2G12. The results demonstrated that once resistance to 2G12 had evolved, viral replication resumed despite MPER antibody treatment without evidence of escape mutations to these MAbs. Manrique et al. (p. 8793–8808), using cell-culture-based systems, now show that resistance to the MPER MAbs is difficult to achieve and can lead to selection of variants with impaired infectivity. This vulnerability of the virus to interference with the MPER supports the importance of this target in vaccine design.

Superior Smallpox Vaccine Candidates with Integrated Interleukin-15

A smallpox vaccine suitable for contemporary populations with greater numbers of immunodeficient individuals is a priority. Perera et al. (p. 8774–8783) report that the integration of the pleotropic cytokine interleukin-15 (IL-15), which is essential for both innate and adaptive immune responses, into the genome of either a Wyeth vaccine strain derived from the Dryvax vaccine or a nonreplicative modified vaccinia virus Ankara strain results in vaccine candidates with superior immunogenicity, durable efficacy, and safety. These IL-15-integrated derivatives hold promise as more efficacious and safe alternatives to the Dryvax vaccine.

Ancestral Center-of-Tree Human Immunodeficiency Virus Type 1 Proteins Are Functional and Immunogenic

The extensive diversity found in human immunodeficiency virus type 1 (HIV-1) vexingly challenges vaccine development. Rolland et al. (p. 8507–8514) developed a phylogenetics-informed algorithm to reconstruct ancestral HIV-1 sequences, called center-of-tree (COT). COT sequences are designed to minimize genetic distances between the antigen and circulating isolates. Computationally derived COT proteins corresponding to HIV-1 subtype B Gag, Tat, and Nef were generated and shown to retain the functionality of the extant proteins and elicited antigen-specific cellular immune responses in mice. This work establishes a new tool for rational vaccine design.

JOURNAL OF VIROLOGY, Aug. 2007, p. 8477–8487 Vol. 81, No. 16
0022-538X/07/$08.00+0 doi:10.1128/JVI.00477-07

Processing of Capsid Protein by Cathepsin L Plays a Crucial Role in Replication of Japanese Encephalitis Virus in Neural and Macrophage Cells[▽]

Yoshio Mori, Tetsuo Yamashita, Yoshinori Tanaka, Yoshimi Tsuda,† Takayuki Abe, Kohji Moriishi, and Yoshiharu Matsuura*

Department of Molecular Virology, Research Institute for Microbial Diseases, Osaka University, Osaka, Japan

Received 6 March 2007/Accepted 25 May 2007

The flavivirus capsid protein not only is a component of nucleocapsids but also plays a role in viral replication. In this study, we found a small capsid protein in cells infected with Japanese encephalitis virus (JEV) but not in the viral particles. The small capsid protein was shown to be generated by processing with host cysteine protease cathepsin L. An in vitro cleavage assay revealed that cathepsin L cleaves the capsid protein between amino acid residues Lys^{18} and Arg^{19}, which are well conserved among the mosquito-borne flaviviruses. A mutant JEV resistant to the cleavage of the capsid protein by cathepsin L was generated from an infectious cDNA clone of JEV by introducing a substitution in the cleavage site. The mutant JEV exhibited growth kinetics similar to those of the wild-type JEV in monkey (Vero), mosquito (C6/36), and porcine (PK15) cell lines, whereas replication of the mutant JEV in mouse macrophage (RAW264.7) and neuroblastoma (N18) cells was impaired. Furthermore, the neurovirulence and neuroinvasiveness of the mutant JEV to mice were lower than those of the wild-type JEV. These results suggest that the processing of the JEV capsid protein by cathepsin L plays a crucial role in the replication of JEV in neural and macrophage cells, which leads to the pathogenesis of JEV infection.

The genus *Flavivirus* within the family *Flaviviridae* comprises over 70 viruses, many of which are predominantly arthropod-borne viruses, such as Japanese encephalitis virus (JEV), West Nile virus (WNV), Murray Valley encephalitis virus (MVE), dengue virus (DEN), yellow fever virus (YFV), and tick-borne encephalitis virus (TBEV). They frequently cause significant morbidity and mortality in mammals and birds (5). JEV is distributed in the south and southeast regions of Asia and is kept in a zoonotic transmission cycle between pigs or birds and mosquitoes (5, 42, 45). JEV spreads to dead-end hosts, including humans, through the bite of JEV-infected mosquitoes and causes infection of the central nervous system with a high mortality rate (5, 45). JEV has a single-stranded positive-strand RNA genome of approximately 11 kb, which is capped at the 5′ end but lacks a 3′ polyadenine tail (24). The ability of the flaviviral genomic RNA to cyclize is crucial for viral replication (1, 14). Among mosquito-borne flaviviruses, two complementary cyclization sequences, mapped in the capsid protein-coding region and 3′ untranslated region (UTR), mediated the cyclization by RNA-RNA base pairing, together with a second pair of complementary sequences, named 5′ and 3′ upstream AUG regions (1, 10, 14, 19, 25). The genomic RNA includes a single large open reading frame, and a polyprotein translated at the endoplasmic reticulum (ER) membrane is cleaved co- and posttranslationally by host and viral proteases to yield three structural proteins, the capsid, precursor membrane (prM), and envelope (E) proteins, and at least seven nonstructural proteins, NS1, NS2A, NS2B, NS3, NS4A, NS4B, and NS5 (24).

Although the capsid protein has very little amino acid homology among flaviviruses—for example, the homologies of the capsid protein of JEV to those of WNV, DEN type 2 (DEN2), and TBEV were only 67%, 33%, and 25%, respectively—the structural properties, such as the hydrophobicity profile, abundance of basic amino acid residues, and secondary and tertiary structures, are well conserved (11, 18, 27). The flavivirus capsid protein commonly contains two hydrophobic sequences in the center and the carboxyl terminus. The latter serves as a signal sequence of prM. The signal/anchor sequence is cleaved off by the viral protease NS2B/3, and this cleavage is required for the subsequent liberation of the amino terminus of prM by the host signal peptidase (26, 43, 49). The mature capsid protein may be associated with the ER membrane through the central hydrophobic region (23, 29). Because the capsid protein has RNA-binding ability via the basic amino acid clusters at its amino and carboxyl termini, it is believed to bind to the genomic RNA to form a nucleocapsid (20). Unlike other envelope viruses, the nucleocapsid structures are rarely found in cells infected with flaviviruses (48), although the nucleocapsid of TBEV can assemble in vitro (21). Therefore, viral assembly is thought to be a coordinated process between the membrane-associated capsid protein and two envelope glycoproteins, prM and E, in the ER membrane.

In conflict with their roles as structural proteins, the capsid proteins of some flaviviruses are localized not only in the cytoplasm but also in the nuclei of the infected cells (4, 28, 32, 44, 46–48). We previously reported that the JEV capsid protein

* Corresponding author. Mailing address: Department of Molecular Virology, Research Institute for Microbial Diseases, Osaka University, 3-1 Yamada-oka, Suita, Osaka 565-0871, Japan. Phone: 81-6-6879-8340. Fax: 81-6-6879-8269. E-mail: matsuura@biken.osaka-u.ac.jp.
† Present address: Department of Disease Control, Graduate School of Veterinary Medicine, Hokkaido University, Sapporo 060-0818, Japan.
▽ Published ahead of print on 6 June 2007.

has also been detected in both the nucleoli and cytoplasm and that the mutant virus defective in the nuclear localization of capsid protein exhibited impaired viral growth in mammalian cells and neuroinvasiveness in mice (32). Furthermore, we have also reported that the nuclear and cytoplasmic localizations of the JEV capsid protein are dependent on binding to the host nucleolar protein B23 (46). It has been reported that, in addition to the JEV capsid protein, the WNV and DEN capsid proteins bind to several host proteins, such as Jab1, a component of the COP9 signalosome complex (34), the chaperone protein HSP70 (35), and the heterogenous nuclear ribonucleoprotein K (8), to regulate these functions. Recently, Clyde and Harris have shown that the small capsid protein isoform translated from the second AUG codon of the DEN genome by leaky scanning is important for viral replication (9). In this context, these properties of the flaviviral capsid proteins raised the possibility that they play some roles in viral growth as "nonstructural" proteins.

In this study, we detected a small capsid protein in JEV-infected cells, but not in the released viral particles. The small capsid protein has been shown to be generated by host protease cathepsin L. Cathepsin L was capable of cleaving the capsid protein between amino acid residues Lys^{18} and Arg^{19}. Furthermore, we have generated a mutant JEV carrying a capsid protein resistant to cleavage by cathepsin L. The characterization of this mutant JEV indicated that cleavage of the capsid protein by cathepsin L plays important roles in viral replication in mouse neuroblastoma and macrophage cells and in the pathogenesis of encephalitis in vivo. These results suggest a novel mechanism for JEV to adapt host cells by the processing of the capsid protein.

MATERIALS AND METHODS

Cells. The mammalian cell lines Vero (monkey kidney), 293T (human kidney), PK15 (pig kidney), RAW264.7 (mouse macrophage), and N18 (mouse neuroblastoma) were maintained in Dulbecco's modified Eagle's minimal essential medium (DMEM) supplemented with 10% fetal bovine serum (FBS). Mosquito cell line C6/36 (*Aedes albopictus*) was grown in Eagle's minimal essential medium supplemented with 10% FBS. Vero cell lines Vero/siNC and Vero/siCTSL, stably expressing the hairpin small interfering RNAs (siRNA) for the nonsense sequence and cathepsin L, respectively, were established by transfection with plasmids pSilencer/NC and pSilencer/CTSL (see below), respectively, and selected with DMEM containing 10% FBS and 50 μg/ml hygromycin B (Sigma, St. Louis, MO).

Plasmids. The cDNA for the capsid protein of JEV AT31 (amino acid residues 2 to 105) was amplified from pMWATG1 (54) by PCR using Ex-*Taq* (Takara, Shiga, Japan) and cloned between the FLAG and hemagglutinin (HA) tags in pcDNA3.1FlagHA (36). From this plasmid, the capsid cDNAs with or without FLAG and/or HA tags were amplified by PCR and subcloned into a mammalian expression vector pCAGPM (31) and designated pCAG/FLAG-JEC-HA, pCAG/FLAG-JEC, pCAG/JEC-HA, and pCAG/JEC. By the same procedure, the plasmids encoding FLAG- and HA-tagged DEN2 and DEN4 capsid proteins, pCAG/FLAG-DEN2C-HA and pCAG/FLAG-DEN4C-HA, were generated from the plasmids encoding the capsid proteins of DEN2 and DEN4, respectively (the kind gifts from F. Hasebe and M. Tadano, respectively). For mutational analyses of the amino acid residues from 14 to 23 (based on the JEV capsid protein sequence), a series of point mutants of the FLAG- and HA-tagged JEV capsid proteins were synthesized by PCR-based mutagenesis (17). All of the mutant genes, as well as the wild-type gene, were cloned into pCAGPM. The JEV capsid gene was cloned into pcDNA 3.1/myc-His (Invitrogen, Carlsbad, CA), and the cDNA encoding the JEV capsid protein fused with myc and His tags was amplified and cloned into bacterial expression vector pET32a (Merck Novagen, Darmstadt, Germany). The resulting plasmid was designated pET32/JECmycHis. The cDNAs of human cathepsins B and L were amplified from 293T cells by reverse transcription-PCR and cloned into pcDNA 3.1/myc-His. An enzymatically inactive mutation of cathepsin L in which Cys^{138} was replaced with Ala was generated by PCR-based mutagenesis. Expression vector pSilencer/CTSL, for a hairpin siRNA for African green monkey cathepsin L, was generated by annealing with synthesized nucleotides (sense, GAT CCG GCG ATG CAC AAC AGA TTA TTC AAG AGA TAA TCT GTT GTG CAT CGC CTT TTT TGG AAA; antisense, AGC TTT TCC AAA AAA GGC GAT GCA CAA CAG ATT ATC TCT TGA ATA ATC TGT TGT GCA TCG CCG) and insertion into the BamHI and HindIII sites of p*Silencer* 2.1 U6 hygro (Ambion Inc., Austin, TX). pSilencer/NC, encoding an siRNA with no homology to mammalian genes, was used as a negative control. pMWAT/L17A carrying replacements of cytosine at nucleotide 144 and thymine at nucleotide 145 with guanine and cytosine, respectively, in pMWATG1, an infectious cDNA clone of JEV, was constructed by PCR-based mutagenesis which results in the replacement of Leu^{17} in the capsid protein with Ala (see Fig. 5A). In addition, adenine-to-guanine and guanine-to-cytosine mutations were introduced into pMWATG1 and pMWAT/L17A at nucleotides 10865 and 10866 of the JEV gene, respectively. The resulting plasmids were named pMWAT/CSmt and pMWAT/L17ACSmt, respectively.

Viruses. The wild-type and L17A/CSmt JEVs were generated from plasmids pMWATG1 and pMWAT/L17ACSmt, respectively, by a method described previously (54). The infectivity of the viruses was determined by an immunostaining focus assay as described previously (32) and expressed in focus-forming units (FFU). The JEV particles were purified from the supernatant of the infected Vero cells as described previously with some modifications (32). Briefly, the virions were clarified by centrifugation at 6,000 × *g* for 30 min and precipitated with 10% polyethylene glycol (molecular mass, approximately 6,000 kDa). The precipitates were collected by centrifugation at 10,000 × *g* for 45 min and centrifuged at 147,000 × *g* for 20 h on a 20 to 60% sucrose gradient. The fractions ranging from 1.16 to 1.19 g/ml in gravity were used as the purified virion.

Antibodies. Anti-JEV capsid protein rabbit polyclonal antibody (PAb) was prepared as described previously (32). Monoclonal antibodies (MAbs) to JEV E (10B4) and NS3 proteins (34A1) were generous gifts from E. Konishi and K. Yasui, respectively. Anti-FLAG tag (M2) and anti-β-actin MAbs were purchased from Sigma. Anti-HA (HA11) and anti-myc tag (9E10) MAbs were purchased from Covance (Richmond, CA). An antinucleolin MAb (MS-3) was purchased from Santa Cruz Biotechnology (Santa Cruz, CA). Anti-PA28-alpha and anti-cathepsin L rabbit PAbs were purchased from Affinity Bioreagents (Golden, CO) and Merck Calbiochem (Darmstadt, Germany), respectively.

Infection, transfection, immunoblotting, and cell fractionation. A monolayer of Vero or N18 cells was infected at multiplicities of infection (MOI) of 5 and 10 with the wild-type and L17A/CSmt JEVs. Plasmids were transfected by *Trans*IT LT-1 (Mirus, Madison, WI) and Lipofectamine 2000 (Invitrogen) for Vero and 293T cells, respectively, according to the manufacturers' instructions. At 24 h after inoculation or transfection, cells were lysed on ice by Triton lysis buffer (20 mM Tris-HCl [pH 7.4], 135 mM NaCl, 1% Triton X-100, 10% glycerol) supplemented with a protease inhibitor cocktail (Biovision, Mountain View, CA) and subjected to sodium dodecyl sulfate-polyacrylamide gel electrophoresis (SDS-PAGE) and Western blotting as previously described (36, 46). JEV-infected cells were fractionated using a Nuclear/Cytosol Fractionation kit (Biovision).

Inhibition of capsid protein processing. E64d and CA074Me were purchased from the Peptide Institute (Osaka, Japan). Z-Phe-Tyr-(*tert*-butyl)-diazomethyl ketone (DMK) (Z-FY-DMK), Z-Val-Ala-Asp-fluoromethyl ketone (FMK) (Z-VAD-FMK), PD150606, and bafilomycin A1 were purchased from Merck Calbiochem. Chloroquine and ammonium chloride were obtained from Sigma and Nacalai Tesque (Kyoto, Japan), respectively. Chloroquine and ammonium chloride were dissolved in distilled water, and bafilomycin A1 was dissolved in ethanol. The other reagents were dissolved in dimethyl sulfoxide (DMSO). At 24 h after inoculation or transfection, cells were incubated with the culture medium containing each reagent or solvent for 8 h at 37°C and examined by immunoblotting. To determine the effects of CA074Me or FY-DMK on the cleavage of the capsid protein, cells transfected with pCAG/FLAG-JEC-HA were treated with the inhibitor for 8 h at 37°C. The ratios of the densities of the slower- and faster-migrating capsid proteins (C1 and C2, respectively) detected by immunoblotting were calculated by Multi Gauge software (Fujifilm, Tokyo, Japan). The relative cleavage values were determined as the C2 to C1 ratio in the presence of inhibitor/the C2 to C1 ratio in the absence of inhibitor. The inhibitory effects of CA074Me or Z-FY-DMK to cathepsins B and L were determined as described previously (7, 13) with some modifications. Briefly, Vero cells (2×10^5) were treated with CA074Me or Z-FY-DMK for 4 h at 37°C and lysed with 25 μl of acidic lysis buffer consisting of 100 mM sodium acetate (pH 5.0), 1 mM EDTA, 0.5% Triton X-100, 2 mM AEBSF [4-(2-aminoethyl)benzenesulfonyl fluoride] (Merck Calbiochem), 5 μg/ml aprotinin (Nacalai Tesque), 100 μM bestatin (Sigma), and 15 μM pepstatin (Peptide Institute). Insoluble materials

were sedimented in a microcentrifuge at 4°C. Ten microliters of each lysate was mixed with 90 μl of reaction buffer (100 mM sodium acetate [pH 5.0], 1 mM EDTA, 4 mM dithiothreitol, 2 mM AEBSF, 5 μg/ml aprotinin, 100 μM bestatin, 15 μM pepstatin). The resulting samples were mixed with 100 μl of cathepsin B-specific (100 μM Z-Arg-Arg-MCA [4-methylcoumaryl-7-amide; Peptide Institute], 0.1% Brij 35) (3) or cathepsin L-specific (100 μM $[Z\text{-Phe-Arg}]_2$-R110 [Molecular Probes, Eugene, OR], 0.1% Brij 35) (2) substrate solutions in a black 96-well plate (Corning, Corning, NY). After incubation for 30 min at room temperature, fluorescence was measured using a fluorescence multiwell plate reader (CytoFluor 4000 LX1; Applied Biosystems, Foster City, CA) with an excitation of 360 nm and an emission of 460 nm for cathepsin B and with an excitation of 485 nm and an emission of 460 nm for cathepsin L. The relative cleavage value in the absence of each inhibitor was defined as 1.

In vitro processing of the JEV capsid protein. The JEV capsid protein fused with thioredoxin and myc-His tags in the N and C termini, respectively, was purified using TALON metal affinity resin (Clontech, Mountain View, CA) from the lysate of *Escherichia coli* transformed by pET32/JECmycHis. The purified protein was dialyzed with acidic dialysis buffer (50 mM sodium acetate [pH 5.5], 1 mM EDTA) for 24 h at 4°C. The recombinant JEV capsid protein (33 μg [1 nmol]/100 μl) was incubated with 0.01 units (170 ng) of human cathepsin L (Merck Calbiochem) for 2 h at room temperature. According to the manufacturer's instructions, one unit is defined as an amount of the enzyme capable of hydrolyzing 1.0 μmol of Z-Phe-Arg-AMC (7-amino-4-methylcoumarin) per minute at 37°C. The resulting samples were subjected to SDS-PAGE and Western blotting using anti-myc MAb. The N-terminal peptide sequences of the cleaved capsid proteins were determined by the Edman degradation method at the APRO Life Science Institute (Tokushima, Japan).

Computer analyses of the flavivirus capsid genes. The amino acid sequences of the flavivirus capsid proteins were aligned with the software package GENETYX-MAC, version 12 (GENETYX, Tokyo, Japan). The GenBank accession numbers of the analyzed sequences are as follows: JEV AT31 strain, AB196923; MVE 1-51 strain, AF161266; WNV IS-98 STD1 strain, AF481864; DEN1 Singapore S275/90 strain, M87512; DEN2 New Guinea C strain, M29095; DEN3 H87 strain, M93130; DEN4 814669 strain, AF326573; YFV 17D strain, X03700. Nucleotides 135 to 152 and bases 10858 to 10875 in the 5′ and 3′ termini, respectively, connected by 8 X nucleotides alternative to bases 153 to 10857, of the wild-type and mutant JEV genomes were applied to GENETYX-MAC to predict RNA secondary structures with minimum free energy.

Growth kinetics of JEVs in vitro. Vero, C6/36, PK15, N18, RAW264.7, Vero/siNC, and Vero/siCTSL cells in 24-well plates (2×10^5) were infected with the wild-type or L17A/CSmt virus at an MOI of 5 for 1 h, washed three times with a medium to remove unbound viruses, and incubated with a medium supplemented with 5% FBS for a total duration of 72 h. To examine the effect of the cathepsin L inhibitor on virus growth, DMSO or 1 μM Z-FY-DMK was added to the culture medium over the incubation period (24 h). The culture supernatants were used for titration of infectious virus.

Mouse experiments. The pathogenicity of JEV to mice was determined as described previously (32). Briefly, 3-week-old female ICR mice were purchased from CLEA Japan (Osaka, Japan) and kept in special pathogen-free environments. Groups of 10 mice were intracerebrally inoculated with 30 μl of 10-fold-diluted solutions of wild-type or L17A/CSmt virus. The virus-diluting solution (DMEM) was administered to two mice as a control. The mice were observed for 2 weeks after inoculation to determine survival rates. The value of the 50% lethal dose (LD_{50}) of each virus was determined by the method by Reed and Müench (39). To examine viral growth in the brain, 100 FFU of the viruses were intracerebrally administered to the mice. At 3 and 5 days after inoculation, the mice were euthanized, and the brains were collected. The infectious titers in the homogenates of the brains were determined in Vero cells as described above. Groups of 10 mice were inoculated intraperitoneally with 1×10^6 FFU (100 μl) of the viruses. The mice were observed for 3 weeks after inoculation to determine survival rates.

RESULTS

JEV-infected cells contained a small capsid protein. Western blotting analyses of Vero cells infected with JEV revealed capsid proteins of 14 and 12 kDa, which were designated C1 and C2, respectively, in contrast to the purified viral particles, in which only C1 was detected (Fig. 1A), indicating that C1 is a mature capsid protein missing a signal sequence of the prM protein. The C2 protein was also detected in the other cell lines examined, and a further processed capsid protein was detected in N18 cells infected with JEV (Fig. 1B). It was shown that the JEV capsid protein is localized in the nuclei as well as in the cytoplasm of the infected cells (32). The C1 and C2 proteins were also detected in both the cytoplasmic and nuclear fractions (Fig. 1C). These results indicate that two forms of the capsid proteins, C1 and C2, are generated in cells infected with JEV, and the larger capsid (C1) is selectively incorporated into the viral particles.

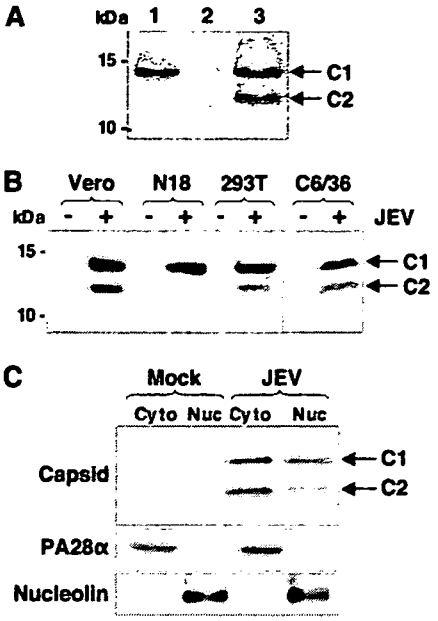

FIG. 1. Detection of C2 protein in cells infected with JEV. (A) Detection of the capsid proteins from the purified viral particles and cells infected with JEV. Lane 1, purified JEV particles produced in Vero cells; lanes 2 and 3, mock- and JEV-infected Vero cells, respectively. Arrows indicate a mature capsid protein (C1) and a further-processed capsid protein (C2). (B) Detection of the capsid protein from various cell lines infected with JEV. (C) Detection of the C1 and C2 proteins in the cytoplasmic (Cyto) and nuclear (Nuc) fractions of Vero cells infected with JEV. PA28-α and nucleolin are control proteins of the cytoplasmic and nuclear fractions, respectively.

The C2 protein lacks the amino terminus. To determine which terminus is missing in the C2 protein, expression plasmids encoding a series of capsid proteins with or without amino-terminal FLAG and carboxyl-terminal HA tags (F-JEC-H, F-JEC, JEC-H, and JEC) were generated (Fig. 2A). Both the C1 and C2 isoforms were detected in Vero cells transfected with each of the expression plasmids by immunoblotting with anti-JEV capsid PAb (Fig. 2B). The size of the C2 proteins in cells transfected with JEC was similar to that of F-JEC, which has the amino-terminal FLAG tag, whereas larger products were detected in the cells transfected with F-JEC-H and JEC-H, which have the carboxyl-terminal HA tag. Consistent with this observation, anti-HA antibody recognized both isoforms in cells expressing F-JEC-H and JEC-H, whereas anti-FLAG antibody detected only C1 in cells expressing F-JEC-H and F-JEC. These results indicate that the C2 protein lacks the amino-terminal region of the JEV capsid protein.

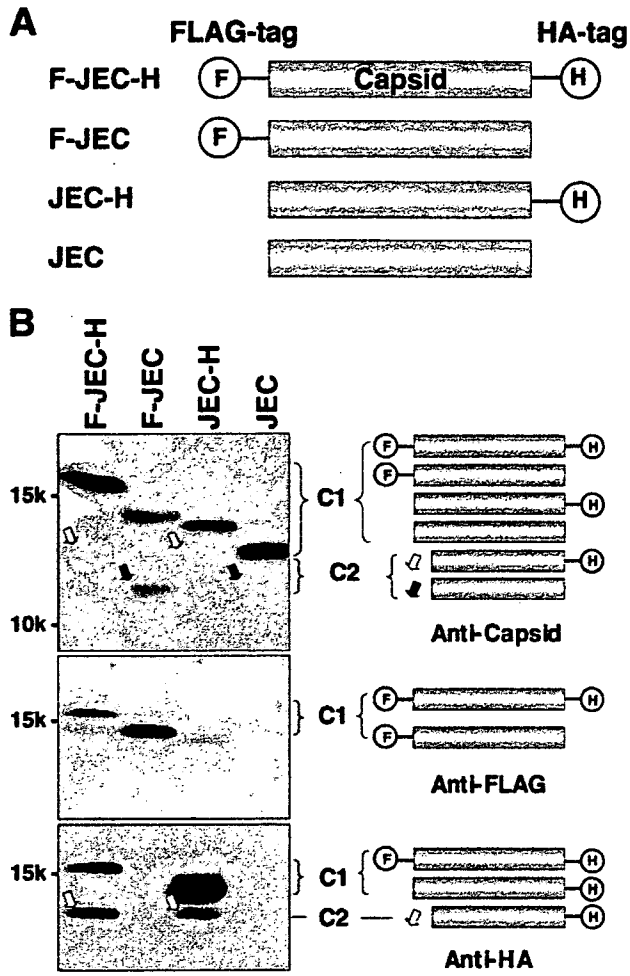

FIG. 2. The C2 protein lacks the amino terminus. (A) Series of the capsid protein constructs with or without FLAG and HA tags in the amino and carboxyl termini, respectively. (B) Expression of a series of the capsid proteins in Vero cells. The cell lysates expressing F-JEC-H, F-JEC, JEC-H, and JEC were examined by immunoblotting using anti-capsid, anti-FLAG, and anti-HA antibodies. The molecules detected by the immunoblotting are indicated on the right. White and black arrows indicate the C2 proteins with and without HA tags in the carboxyl terminus, respectively.

The JEV capsid protein is processed by cathepsin L. The C2 protein missing the amino-terminal region of the JEV capsid protein may be generated through cleavage by a host cell protease(s) or translation from the second start codon by leaky scanning, as reported in the case of DEN2 (9). To assess these possibilities, cells expressing F-JEC-H were treated with various protease inhibitors. C2 production was completely abrogated by treatment with broad-spectrum cysteine protease inhibitor E64d at the concentration of 50 μM, along with an increase in C1 expression (Fig. 3A), indicating that the JEV C2 protein was generated via cleavage of the C1 protein by a cysteine protease(s) but not leaky scanning. To identify the cysteine protease responsible for the processing of the JEV capsid protein, specific inhibitors for individual cysteine proteases were examined in cells expressing F-JEC-H. The inhibitors for cathepsins B and L, CA074Me (10 μM) (6) and Z-FY-DMK (10 μM) (40), impaired the processing, while an inhibitor of caspases, Z-VAD-FMK (20 μM), and an inhibitor of calpains, PD150606 (20 μM), exhibited no effect (Fig. 3A). Cathepsins B and L are known to be present in the late endosome and lysosome. The treatments with inhibitors of these acidic compartments, ammonium chloride (10 mM), chloroquine (50 μM), and bafilomycin A1 (100 nM), also blocked the processing of the capsid protein (Fig. 3B). To determine whether cathepsin B or L is a dominant protease for cleavage of the JEV capsid protein, the dose dependency of the effects of cathepsin inhibitors CA074Me and Z-FY-DMK on the cleavage of F-JEC-H was examined. The processing of the JEV capsid protein was inhibited in a manner that correlated closely with the inactivation of cathepsin L rather than that of cathepsin B (Fig. 3C). Furthermore, overexpression of cathepsin L, but not cathepsin B and inactive cathepsin L (C138A), resulted in an increase of C2 production in 293T cells (Fig. 3D). In addition, production of C2 from F-JEC-H was significantly decreased in two independent clones of Vero cells stably expressing siRNA for cathepsin L (Fig. 3E). These results indicate that cathepsin L is responsible for the processing of the JEV capsid protein to generate the C2 protein.

Identification of the site of the cleavage of the JEV capsid protein by cathepsin L. To determine the site of the cleavage of the JEV capsid protein by cathepsin L, a recombinant capsid protein possessing amino-terminal thioredoxin, His, and S tags and carboxyl-terminal myc and His tags was prepared (Fig. 4A). The in vitro incubation of the purified capsid protein with cathepsin L at room temperature for 60 min generated two major cleaved products, detectable by anti-myc antibody (Fig. 4B). The amino-terminal amino acid sequencing revealed that the mass of cleaved product 1 contained two peptides beginning with the residues Ser-Asp-Lys-Ile-Ile (a minor peptide) and Arg-Gln-His-Met-Asp (a major peptide), corresponding to a region of the thioredoxin and S tags, respectively (Fig. 4A and B). On the other hand, cleaved product 2 contained a single peptide beginning with Arg-Gly-Leu-Pro-Arg, corresponding to amino acid residues 19 to 23 of the JEV capsid protein. This result indicates that the JEV capsid protein is cleaved between Lys^{18} and Arg^{19} by cathepsin L in vitro (Fig. 4C). To further confirm the cleavage of the capsid protein in mammalian cells, a series of F-JEC-H proteins with alanine substitutions in each residue around the cleavage site (Ile^{14} to Arg^{23}) was expressed in Vero cells (Fig. 4D). As indicated in the reports that a hydrophobic amino acid residue at position P2 is responsible for the substrate specificity of cathepsin L (37, 38), the replacement of Leu^{17} (P2) with alanine was crucial for capsid protein processing. In addition, although the single replacements at the cleavage site of Lys^{18} (P1) and Arg^{19} (P1′) with alanine had no effect on cleavage, the double substitution of acidic amino acids (Lys^{18} to Glu and Arg^{19} to Asp) resulted in impairment of C2 production (Fig. 4D). These results indicate that the JEV capsid protein is cleaved between Lys^{18} and Arg^{19} by cathepsin L in vitro and in vivo.

Production of the C2 proteins of DENs. The P4 to P1′ region of the cathepsin L cleavage site is conserved among many mosquito-borne flaviviruses, including MVE, WNV, and DENs (Fig. 4C), and the 5′-complementary cyclization sequences are over-

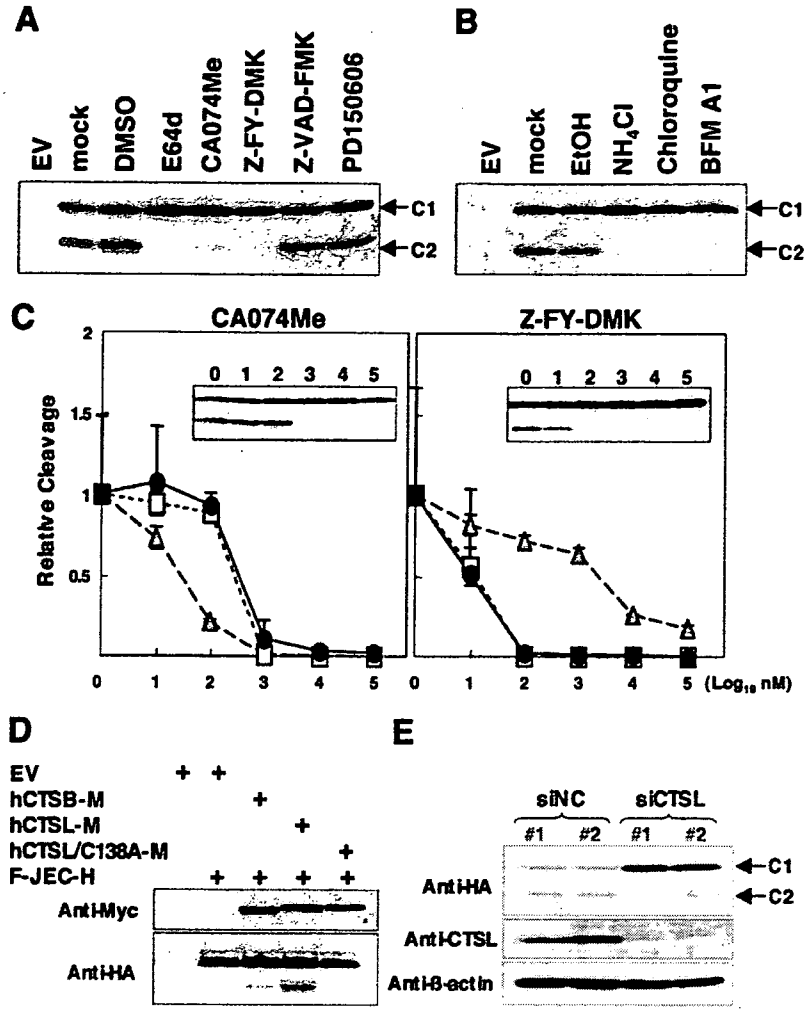

FIG. 3. JEV capsid protein is processed by cathepsin L. (A) Effects of cysteine protease inhibitors on the processing of the JEV capsid protein. Vero cells expressing F-JEC-H were treated with 50 μM E64d, 10 μM CA074Me, 10 μM Z-FY-DMK, 20 μM Z-VAD-FMK, or 20 μM PD150606 for 8 h at 37°C and examined by immunoblotting using an anti-HA antibody. EV, empty vector. (B) Effects of anti-acidic compartment reagents on the processing of the JEV capsid protein. Vero cells expressing F-JEC-H were treated with 10 mM ammonium chloride, 50 μM chloroquine, or 100 nM bafilomycin A1 (BFM A1) for 8 h at 37°C and examined by immunoblotting using an anti-HA antibody. EtOH, ethanol. (C) Dose-dependent effects of two cathepsin inhibitors, CA074Me and Z-FY-DMK, on F-JEC-H processing. Vero cells expressing F-JEC-H were treated with CA074Me or Z-FY-DMK at the indicated concentrations for 8 h at 37°C and examined by immunoblotting using an anti-HA antibody. The relative cleavage values for the capsid protein (solid circles) were calculated as the intensity of C2 compared to that of C1 in three independent experiments. A representative image of the immunoblotting is indicated in each graph panel. The relative levels of cleavage of the substrates specific to cathepsin B (gray triangles) and cathepsin L (open squares) were determined as described in Materials and Methods. The value for the control sample without treatment of each inhibitor was taken as 1. (D) Effects of the overexpression of cathepsins on the processing of the JEV capsid protein. 293T cells were cotransfected with plasmids encoding myc-tagged human cathepsin B (hCTSB-M), cathepsin L (hCTSL-M), or inactive cathepsin L (hCTSL/C138A-M) with F-JEC-H. Immunoblot analysis was carried out using the antibodies shown at the left. (E) Processing of F-JEC-H in Vero cells stably expressing hairpin siRNA corresponding to the negative control (siNC) or cathepsin L (siCTSL). Immunoblot analysis was carried out using the antibodies shown at the left.

lapped through the P4 to P2 sites (1, 19) (Fig. 5A). The C2 proteins were also detected in cells expressing the capsid proteins of DEN2 and DEN4 (Fig. 4E). To determine whether the C2 proteins of DEN are generated in the same manner as the C2 proteins of JEV, we examined the effect of the cysteine protease inhibitor E64d on the productions of the DEN C2 proteins. When cells were treated with E64d at a concentration of 50 μM, the C2 protein was diminished in cells expressing the capsid protein of JEV, but not in those expressing DEN2 and DEN4. However, it should be noted that treatment with the inhibitor induced a slight delay in migration of the C2 proteins of DENs. These results suggest that cysteine proteases do not play a major role in the production of the C2 proteins of DENs but play some roles in their processing.

Construction of a mutant JEV carrying the capsid protein resistant to cleavage by cathepsin L. To assess the biological significance of the cleavage of the JEV capsid protein by cathepsin L, a mutant JEV with Leu^{17} replaced by Ala (L17A)

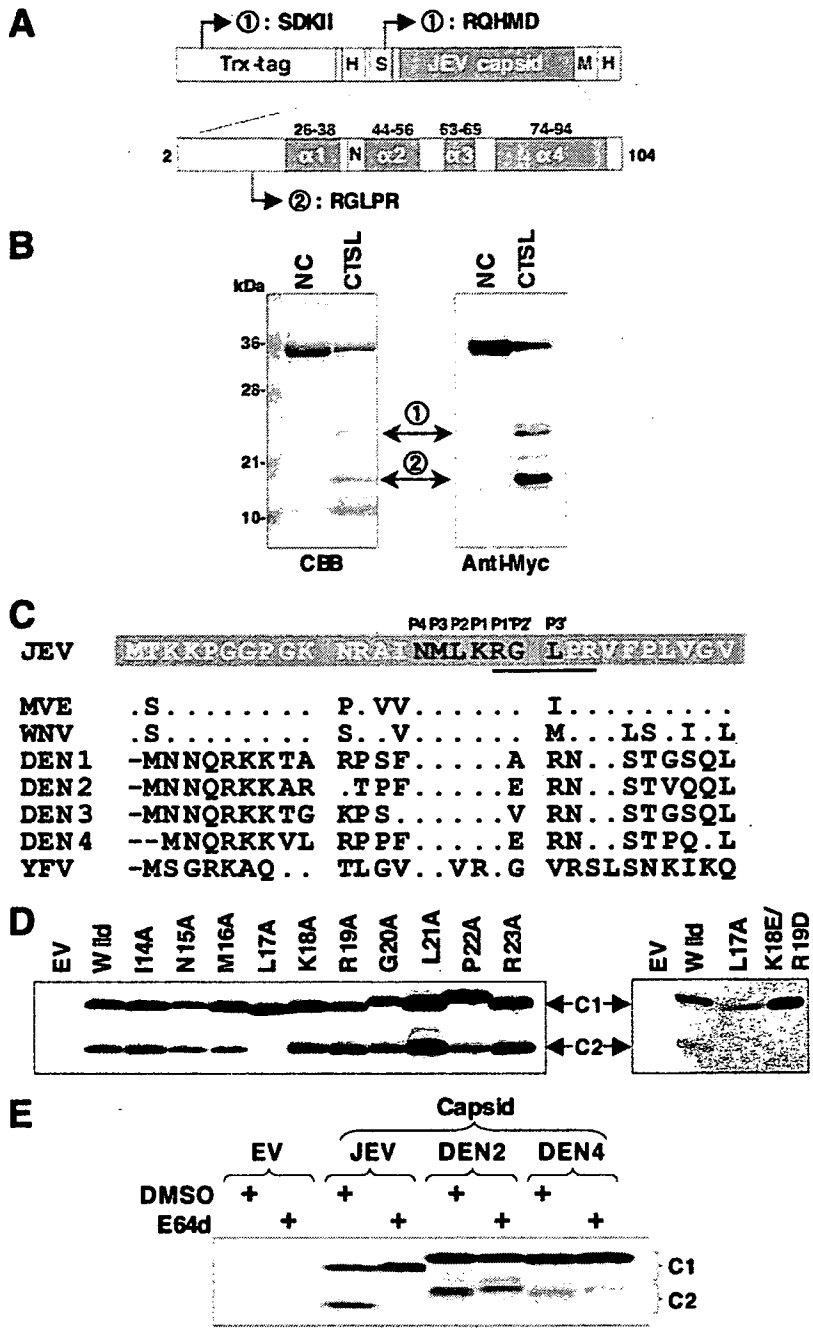

FIG. 4. Identification of the site of cleavage of JEV capsid protein by cathepsin L. (A) Schematic diagram of the recombinant JEV capsid protein. The His, S, and myc tags are indicated as H, S, and M, respectively. Four α-helices (α1 to 4) of the JEV capsid protein were predicted by Ma et al. (27). The nuclear localization signal (N) was mapped to residues Gly[42] and Pro[43] (32). Products 1 and 2 of in vitro cleavage by cathepsin L began at the indicated positions. Trx, thioredoxin. (B) The purified capsid protein (33 μg [1 nmol]/100 μl) was treated with 0.01 units of recombinant human cathepsin L (CTSL) at room temperature for 60 min and analyzed by Coomassie brilliant blue (CBB) staining and immunoblotting using an anti-myc antibody after SDS-PAGE. The amino-terminal amino acid sequences of cleavage products 1 and 2 were determined by the Edman degradation method. (C) Alignment of the amino-terminal amino acid sequences of the mosquito-borne flaviviral capsid proteins. Positions P4 to P3′ of the site of cleavage of the JEV capsid protein by cathepsin L are shown at the top of the sequences. The amino-terminal amino acid sequences of cleavage product 2 generated by cathepsin L in vitro are underlined. Identical and deleted residues compared with the JEV capsid protein are indicated as dots and bars, respectively. (D) Identification of crucial residues for capsid protein processing by cathepsin L in vivo. A series of the mutant constructs derived from F-JEC-H were expressed in Vero cells and analyzed by immunoblotting using an anti-HA antibody. (E) Effect of a cysteine protease inhibitor E64d on the processing of the DEN capsid proteins. Vero cells expressing the FLAG- and HA-tagged capsid proteins of JEV, DEN2, and DEN4 were treated with DMSO or 50 μM E64d for 8 h at 37°C and examined by immunoblotting using an anti-HA antibody.

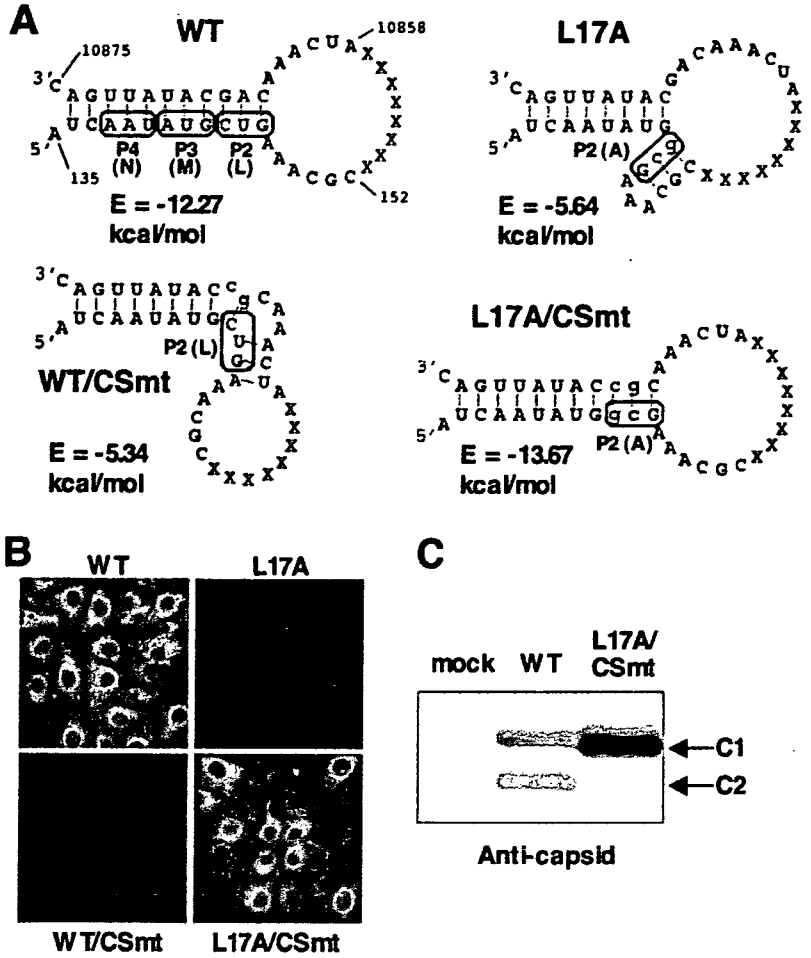

FIG. 5. Construction of a mutant JEV carrying the capsid protein resistant to cleavage by cathepsin L. (A) Predicted RNA secondary structures of the wild-type (WT) and mutant viral genomes. Nucleotides 135 to 152 and bases 10858 to 10875 in the 5′ and 3′ termini, respectively, connected by 8 nonsense nucleotides (X) alternative to bases 153 to 10857, were applied to the computer program GENETYX-MAC, version 12, to calculate free energies (E). The secondary RNA structures with minimum free energies are illustrated. RNA sequences encoding Asp^{15} (P4), Met^{16} (P3), and Leu^{17} (P2) in the 5′ cyclization sequences of the WT JEV, Leu^{17} (P2) for WT/CSmt, and Ala^{17} (P2) for L17A and L17A/CSmt are boxed. The mutated nucleotides are shown by lowercase letters. (B) Vero cells (5×10^6) were electroporated with 10 μg of in vitro-transcribed genomic RNA of WT, L17A, WT/CSmt, or L17A/CSmt virus and immunostained with an anti-E antibody at 4 days posttransfection. (C) Expression of capsid proteins in cells infected with WT or L17A/CSmt JEV. Vero cells were inoculated with the JEVs at an MOI of 10 and analyzed by immunoblotting with anticapsid antibody at 1 day postinfection.

was generated (Fig. 5A). However, the electroporation of the mutant RNA did not result in the production of the viral antigen (Fig. 5B) and infectious particles (data not shown). The coding region for Leu^{17} slightly overlaps the 5′ cyclization sequences, suggesting that the lack of replication of the L17A mutant is caused by the unstable and inappropriate secondary structure of viral RNA (Fig. 5A). To examine this possibility, L17A/CSmt, carrying additional complementary mutations in the 3′ UTR, which was predicted to have a stable secondary structure, and WT/CSmt, carrying a mutation only in the 3′ UTR as a control, were generated (Fig. 5A). Upon electroporation of the genomic RNAs into Vero cells, RNA of L17A/CSmt but not of WT/CSmt exhibited replication (Fig. 5B). As we expected, the C2 protein was not detected in Vero cells infected with L17A/CSmt (Fig. 5C). These results further confirm that RNA-RNA base pairing mediated by the two complementary cyclization sequences in the capsid coding region and 3′ UTR is required for replication of JEV.

Involvement of capsid protein cleavage on the cell type-specific replication of JEV. To examine the biological function of the C2 protein, the growth kinetics of the mutant L17A/CSmt was examined in several cell lines. As shown in Fig. 6A, L17A/CSmt was comparably replicated in Vero, C6/36, and PK15 cells compared with wild-type JEV, whereas growth of L17A/CSmt was 3.3- to 6.1-fold lower and 10.8- to 11.8-fold lower than that of wild-type JEV in N18 and RAW264.7 cells, respectively. In addition, L17A/CSmt exhibited reduced synthesis of the viral protein in N18 cells but not in Vero cells (Fig. 6B), suggesting that impairment of L17A/CSmt replication in N18 cells might be attributable to the reduction of viral protein synthesis. To further confirm the involvement of capsid protein cleavage in the cell type-specific restriction of L17A/CSmt rep-

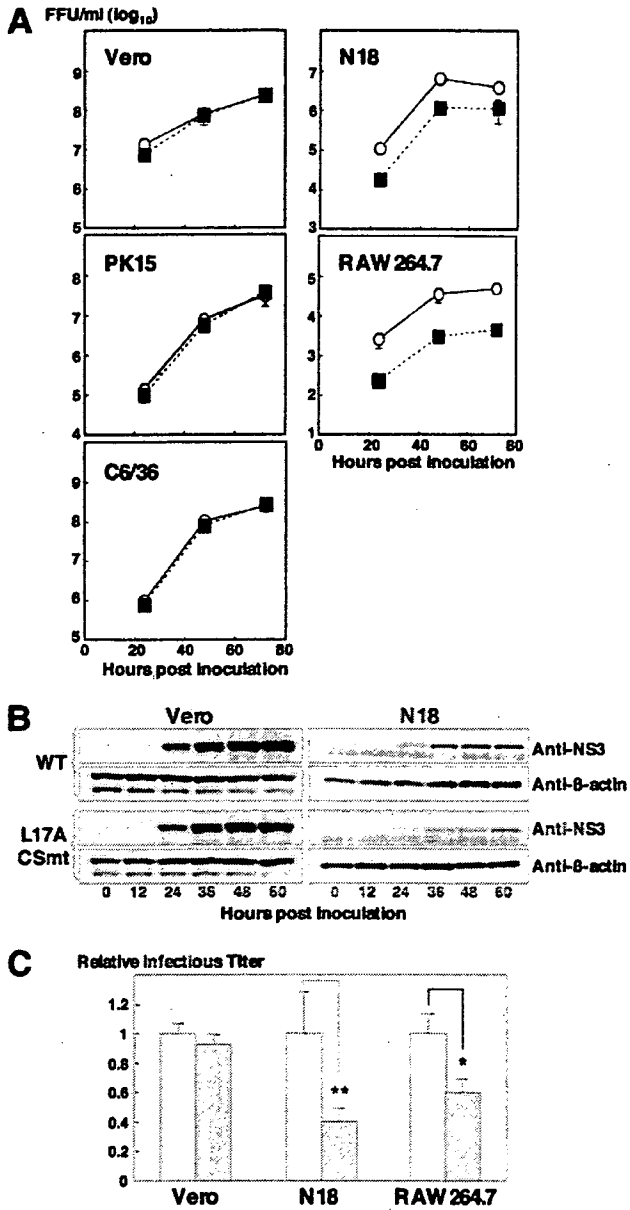

FIG. 6. Growth kinetics of L17A/CSmt in various cell lines. (A) The wild-type (WT; open circles) and mutant L17A/CSmt (solid squares) JEVs were inoculated into Vero, C6/36, PK15, N18, and RAW264.7 cells at an MOI of 10. After the indicated times, the infective titers in the culture supernatants on Vero cells were determined. (B) Viral protein synthesis in Vero and N18 cells infected with the WT or L17/CSmt virus. The NS3 and β-actin proteins were detected by immunoblotting with anti-JEV NS3 and anti-β-actin MAbs, respectively. (C) The WT JEV was inoculated into Vero, N18, and RAW264.7 cells at an MOI of 10 and incubated in the presence of DMSO (white bars) or 1 μM Z-FY-DMK (gray bars). At 24 h after inoculation, the infectious titers in the culture supernatants on Vero cells were determined. Asterisks showed significant differences by *t* test (**, $P < 0.01$; *, $P < 0.05$).

lication, we examine the effect of the cathepsin L inhibitor on JEV replication. The cathepsin L inhibitor suppressed the growth of the wild-type virus in N18 and RAW264.7 cells, but not in Vero cells (Fig. 6C). Furthermore, the wild-type virus

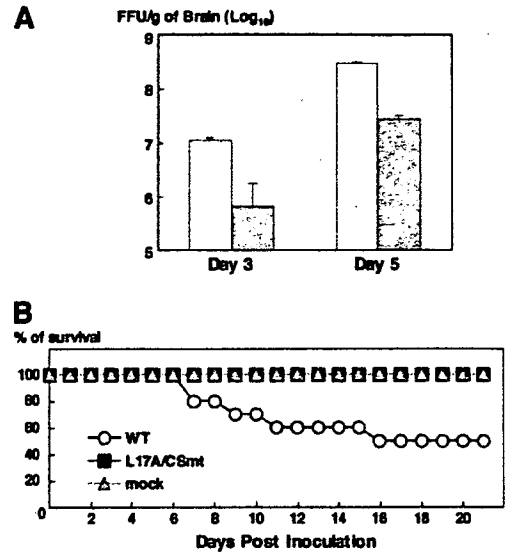

FIG. 7. Neurovirulence and neuroinvasiveness of L17A/CSmt in mice. (A) Growth of the wild-type (WT; white bars) and mutant L17A/CSmt (gray bars) virus in mouse brain. One hundred FFU of each virus were intracerebrally injected into 3-week-old ICR mice, and the progeny viruses in the brain at 3 or 5 days after inoculation on Vero cells were determined. (B) Neuroinvasiveness of the WT and mutant JEVs to mice. Ten ICR mice were intraperitoneally inoculated with 1×10^6 FFU of each virus, and the survival rates of the mice were determined for 21 days.

replicated equally in Vero/siNC and Vero/siCTSL cells (data not shown). These results suggest that generation of the C2 protein is required for the efficient replication of JEV in murine macrophage and neural cells.

Neurovirulence and neuroinvasiveness of L17A/CSmt in mice. To compare the levels of neurovirulence of the wild-type and mutant viruses, we determined the LD_{50} values by intracerebral inoculation of the viruses in 3-week-old ICR mice. The LD_{50} value of L17A/CSmt (12.3 FFU) was approximately five times higher than that of the wild-type JEV (2.7 FFU). Although no significant difference in symptoms was observed between mice inoculated with 100 FFU of the wild-type and the mutant viruses, L17A/CSmt required longer periods than the wild-type JEV to kill mice (wild type versus L17A/CSmt: 6.8 ± 0.9 versus 8.4 ± 1.4 days postinoculation). To examine the growth kinetics of the viruses in the mouse brain, 100 FFU of each virus were intracerebrally injected and the progeny viruses in the brain were determined. The growth of L17A/CSmt was 16.3 and 11.0 times lower than that of the wild-type virus at 3 and 5 days after inoculation, respectively (Fig. 7A). Next, to compare the levels of neuroinvasiveness of the wild-type and mutant viruses, ICR mice were intraperitoneally inoculated with 1×10^6 FFU of each virus. All of the 10 mice inoculated with L17A/CSmt survived, whereas one-half of the mice inoculated with the wild-type JEV died by 10.0 days postinoculation on average (Fig. 7B). These results indicated that the L17A/CSmt mutant resistant to the cleavage by cathepsin L exhibits impaired neurovirulence and neuroinvasiveness in mice.

DISCUSSION

Posttranslational modifications, including proteolysis, glycosylation, and phosphorylation, play a key role in regulating the functions of various proteins. Flavivirus proteins are translated as a single large precursor polyprotein, and proteolysis by host and viral proteases, such as signal peptidase, NS2B/3, and furin, is crucial for viral propagation (24). In this study, we demonstrate that some fraction of the mature JEV capsid proteins (C1) are further processed into a small form of capsid protein (C2) by cathepsin L, a papain-like cysteine protease. Furthermore, the C2 protein was shown to play a role in the replication of JEV in neural and macrophage cells and pathogenicity in mice. It is well established that cathepsins, a large group of lysosomal proteases, are involved in the bulk degradation of proteins in the lysosome. On the other hand, limited proteolysis by cathepsins has also been shown to convert a hormone (12), a neurotransmitter (51), and transactivators (15, 16, 33) from inactive precursors to the active forms and facilitate entry of several viruses (7, 13, 41).

It has been shown that the JEV C2 protein can be generated by the cleavage of the amino-terminal 18 amino acids from the C1 capsid protein by cathepsin L. However, the amino-terminal part of the cleavage product was not detected even though a FLAG tag was added (Fig. 2B). Therefore, the fate of the N-termimal 18 residues is currently unknown. The C2 protein was detected only in the cells, not in the viral particles, in contrast to the C1 protein, which was detected in both. The amino-terminal 32 amino acids and carboxyl-terminal 26 amino acids of the capsid protein of Kunjin virus (KUN), an Australian subtype of WNV, are essential for binding to the genomic RNA (20). The amino-terminal region of the capsid protein is well conserved between JEV and WNV. Therefore, it is possible that the JEV C2 protein is not incorporated into viral particles due to lack of the amino-terminal region of the capsid protein, required for binding to the viral RNA. Three-dimensional structural analyses revealed that the DEN and KUN capsid proteins contain four α-helixes and form a homodimer and a homotetramer (11, 27), and the amino-terminal 20 amino acids of the DEN capsid protein were shown to be flexible and not resolvable by nuclear magnetic resonance assay (27). In addition, a deletion mutant of the capsid protein of KUN lacking the amino-terminal 22 amino acids was used to determine the crystal structure (11). Therefore, the amino-terminal region of the flaviviral capsid proteins might not be involved in the self-assembly of the capsid proteins.

The capsid proteins in the fraction that are degraded rather than secreted as virions are likely to come in contact with cathepsin L in the acidic compartments such as the lysosome. Furthermore, subcellular fractionation indicated that the C2 protein had also migrated into the nucleus after processing. Our previous studies have shown that nuclear localization of the capsid protein and binding with the host nucleolar protein B23 are important for JEV replication (32, 46). These data suggest that the JEV capsid protein is translocated from the cytoplasm to the nucleus through the acidic compartment. Although the trafficking mechanisms of the capsid protein remain unknown, the C2 protein is able to migrate into the nucleus through the nuclear localization signal and B23-binding domain at Gly^{42} and Pro^{43} (32, 46). The C2 protein of a mutant JEV in which Gly^{42} and Pro^{43} were replaced with alanines (32) was impaired in nuclear localization, and the mutant capsid protein missing the amino-terminal amino acids was detected in the nucleus, especially in the nucleolus, when it was expressed by plasmid transfection (data not shown). On the other hand, it has been reported that cathepsin L or a cathepsin L-like protease is expressed in the nucleus and cleaves some host proteins, such as CDP/Cux (16), RB, and SP-1 (15, 33). Therefore, the JEV capsid protein might be alternatively processed in the nucleus by the proteases. In the case of WNV, the export of the capsid protein from the nucleus was facilitated in a Jab1-binding manner (34), and the Jab1-binding motif (Pro-Gly-Gly-Pro; residues 5 to 8) was also conserved in the JEV capsid protein. Therefore, the C2 protein lacking the Jab1-binding motif due to cleavage with cathepsin L might be able to escape from Jab1-dependent nuclear export and accumulate in the nucleus.

It has been established that the primary determinants of the specificity for cathepsin L are the S2 subsite (as shown in other papain-like proteases) and the hydrophobic residues at the P2 position of the substrates (37, 38). In addition, basic residues show a preference for the P1 position of substrates (38). These properties are in good agreement with our results that the cleavage site of the JEV capsid protein by cathepsin L is between Lys^{18} and Arg^{19} and that Leu^{17} at the P2 site was crucial for the cleavage. The residues P4 to P1′ are well conserved among mosquito-borne flaviviruses except for YFV, and the amino acid changes of the YFV capsid protein occur only within hydrophobic (Leu to Val at the P2 site) and basic (Lys to Arg at the P1 site) residues, respectively (Fig. 4C). Therefore, the capsid protein of YFV may also be cleaved by cathepsin L.

On the other hand, it has been reported that a small capsid protein of DEN2 was generated by leaky scanning (9). Due to the lack of a Kozak consensus sequence around the first start codon in many mosquito-borne flaviviruses, including DEN2, the smaller capsid protein of DEN2 is translated from the second or third AUG codon (9). In this context, two independent mechanisms of leaky scanning and processing by cathepsin L might be involved in the production of the small capsid protein. If both mechanisms were involved in the processing of the capsid protein of DEN, the C2 products that were generated by leaky scanning that started at residue Met^{15} and then were processed by cathepsin L at Arg^{18} should be present. This hypothesis is supported by the detection of the slowly migrating C2 proteins of DEN2 and -4 by SDS-PAGE due to treatment with E64d (Fig. 4E). The fast-migrating forms of the C2 proteins of DEN2 and -4 may be generated by cleavage by cathepsin L, while the slowly migrating forms detected in the presence of the inhibitor may be generated by leaky scanning. In contrast, the JEV genome possesses the ideal Kozak consensus sequence around the first AUG codon (9), and thus leaky scanning should not be involved in the production of the C2 protein.

Generation of the L17A capsid mutant in combination with the changes in the CSmt region (L17A/CSmt mutant) was necessary to ensure that altering the Leu^{17} codon did not also affect the 3′ cyclization sequence essential for viral replication. The RNA-RNA interaction between the 5′ cyclization sequences, in which the conserved amino acids required for ca-

thepsin L cleavage are partially encoded, and the 3′ cyclization sequences was predicted for the flaviviruses (19), and the importance of the interaction for replication has been demonstrated in many flaviviruses (1, 10, 14, 19, 25). In this study we further confirmed the crucial role of the interaction of both the 5′ and 3′ ends of the viral RNA for JEV replication. Replication is a prerequisite for the viral life cycle; therefore, the capacity for the processing of the capsid protein, which is partially encoded in the 5′ cyclization sequences, by cathepsin L should be acquired during the viral adaptation to the hosts.

The growth kinetics of the L17A/CSmt JEV was reduced in RAW264.7 and N18 cells, but not in Vero, PK15, and C6/36 cells. It is noteworthy that the neural cells and the cells of monocyte/macrophage lineage are known to support JEV replication in vivo (22, 30, 50). The present study could not completely exclude the possibility that the complementary mutations in the cyclization sequences and/or the structure of the mutant capsid protein may be responsible for the reduced replication of the mutant virus in specific cells in culture or in vivo. It has been previously reported that DEN RNA with complementary mutations in the cyclization sequences recovered its direct interaction and self-primed RNA synthesis to the same level as seen in the wild-type RNA in a cell-free system (52, 53), whereas similar mutations significantly delayed RNA replication of the KUN replicon (19). Suppression of viral replication in N18 and RAW264.7 cells by treatment with the cathepsin L inhibitor further supports the possibility that the cleavage of capsid protein rather than RNA alteration in the cyclization sequences plays a crucial role in viral replication. Generation of the C2 protein is not a prerequisite for the cell-specific replication of JEV, because the processing of the capsid protein by cathepsin L was observed in all of the cells examined. However, we do not know the reason why the cell lines that showed the lowest production of the C2 protein exhibited the lowest viral production and the largest difference in growth of wild-type and L17A/Csmt viruses at the moment. Interaction of the C2 protein with a host factor(s) may be required for efficient replication of JEV in neural and macrophage cells, in which virus replicates at a low level, whereas the C2 protein may be unnecessary for replication in highly replication-competent cells, such as Vero, C6/36, and PK15 cells. The importance of the small capsid protein for viral replication has been shown in a study of DEN2, but a cell tropism for viral replication has not been reported (9).

Consistent with the data obtained in vitro, the L17A/CSmt mutant exhibited slow growth in the mouse brain. In addition, the limited growth of the mutant JEV in RAW264.7 and N18 cells may be a reflection of its reduced neuroinvasiveness. The symptoms of mice intracerebrally inoculated with the L17A/CSmt mutant were indistinguishable from those inoculated with the wild type, although disease induction required more time and a larger amount of virus than that due to inoculation with the wild type. These results suggest that the C2 protein is involved in viral replication in vivo but does not directly participate in virulence. This is in clear contrast to the mutant JEV defective in the nuclear localization of the capsid protein, which exhibited neurovirulence comparable to that of the wild type in spite of severe impairment of growth in the brain (32).

The present study demonstrated that cleavage of the capsid protein by cathepsin L and the resulting C2 protein missing the amino-terminal 18 amino acids plays a role in JEV replication in the nerve and macrophage cell lines, suggesting that the capsid protein has additional functions other than nucleocapsid formation. The limited genomic information of flaviviruses may constrain the multiassignment strategies of the viral proteins during the evolutional adaptation of the viruses to their hosts.

ACKNOWLEDGMENTS

We thank H. Murase for her secretarial work. We also thank T. Wakita for providing the JEV infectious clone plasmids, E. Konishi and K. Yasui for the gifts of the anti-E and NS3 antibodies, respectively, and F. Hasebe and M. Tadano for the plasmids encoding the DEN2 and DEN4 capsid proteins, respectively.

This research was supported in part by grants-in-aid from the Ministry of Health, Labor, and Welfare; the Ministry of Education, Culture, Sports, Science, and Technology; the 21st Century Center of Excellence Program; the Foundation for Biomedical Research and Innovation; and the Zoonoses Control Project of the Ministry of Agriculture, Forestry and Fisheries of Japan.

REFERENCES

1. **Alvarez, D. E., M. F. Lodeiro, S. J. Luduena, L. I. Pietrasanta, and A. V. Gamarnik.** 2005. Long-range RNA-RNA interactions circularize the dengue virus genome. J. Virol. **79**:6631–6643.
2. **Assfalg-Machleidt, I., G. Rothe, S. Klingel, R. Banati, W. F. Mangel, G. Valet, and W. Machleidt.** 1992. Membrane permeable fluorogenic rhodamine substrates for selective determination of cathepsin L. Biol. Chem. Hoppe-Seyler. **373**:433–440.
3. **Barrett, A. J., and H. Kirschke.** 1981. Cathepsin B, cathepsin H, and cathepsin L. Methods Enzymol. **80**:535–661.
4. **Bulich, R., and J. G. Aaskov.** 1992. Nuclear localization of dengue 2 virus core protein detected with monoclonal antibodies. J. Gen. Virol. **73**:2999–3003.
5. **Burke, D. S., and T. P. Monath.** 2001. Flaviviruses, p. 1043–1125. *In* D. M. Knipe, P. M. Howley, D. E. Griffin, R. A. Lamb, M. A. Martin, B. Roizman, and S. E. Straus (ed.), Fields virology, 4th ed., vol. 1. Lippincott Williams & Wilkins, Philadelphia, PA.
6. **Buttle, D. J., M. Murata, C. G. Knight, and A. J. Barrett.** 1992. CA074 methyl ester: a proinhibitor for intracellular cathepsin B. Arch. Biochem. Biophys. **299**:377–380.
7. **Chandran, K., N. J. Sullivan, U. Felbor, S. P. Whelan, and J. M. Cunningham.** 2005. Endosomal proteolysis of the Ebola virus glycoprotein is necessary for infection. Science **308**:1643–1645.
8. **Chang, C. J., H. W. Luh, S. H. Wang, H. J. Lin, S. C. Lee, and S. T. Hu.** 2001. The heterogeneous nuclear ribonucleoprotein K (hnRNP K) interacts with dengue virus core protein. DNA Cell Biol. **20**:569–577.
9. **Clyde, K., and E. Harris.** 2006. RNA secondary structure in the coding region of dengue virus type 2 directs translation start codon selection and is required for viral replication. J. Virol. **80**:2170–2182.
10. **Corver, J., E. Lenches, K. Smith, R. A. Robison, T. Sando, E. G. Strauss, and J. H. Strauss.** 2003. Fine mapping of a *cis*-acting sequence element in yellow fever virus RNA that is required for RNA replication and cyclization. J. Virol. **77**:2265–2270.
11. **Dokland, T., M. Walsh, J. M. Mackenzie, A. A. Khromykh, K. H. Ee, and S. Wang.** 2004. West nile virus core protein; tetramer structure and ribbon formation. Structure **12**:1157–1163.
12. **Dunn, A. D., H. E. Crutchfield, and J. T. Dunn.** 1991. Thyroglobulin processing by thyroidal proteases. Major sites of cleavage by cathepsins B, D, and L. J. Biol. Chem. **266**:20198–20204.
13. **Ebert, D. H., J. Deussing, C. Peters, and T. S. Dermody.** 2002. Cathepsin L and cathepsin B mediate reovirus disassembly in murine fibroblast cells. J. Biol. Chem. **277**:24609–24617.
14. **Filomatori, C. V., M. F. Lodeiro, D. E. Alvarez, M. M. Samsa, L. Pietrasanta, and A. V. Gamarnik.** 2006. A 5′ RNA element promotes dengue virus RNA synthesis on a circular genome. Genes Dev. **20**:2238–2249.
15. **Fu, Y. H., T. Nishinaka, K. Yokoyama, and R. Chiu.** 1998. A retinoblastoma susceptibility gene product, RB, targeting protease is regulated through the cell cycle. FEBS Lett. **421**:89–93.
16. **Goulet, B., A. Baruch, N. S. Moon, M. Poirier, L. L. Sansregret, A. Erickson, M. Bogyo, and A. Nepveu.** 2004. A cathepsin L isoform that is devoid of a signal peptide localizes to the nucleus in S phase and processes the CDP/Cux transcription factor. Mol. Cell **14**:207–219.
17. **Higuchi, R., B. Krummel, and R. K. Saiki.** 1988. A general method of in vitro preparation and specific mutagenesis of DNA fragments: study of protein and DNA interactions. Nucleic Acids Res. **16**:7351–7367.

18. **Jones, C. T., L. Ma, J. W. Burgner, T. D. Groesch, C. B. Post, and R. J. Kuhn.** 2003. Flavivirus capsid is a dimeric alpha-helical protein. J. Virol. 77:7143–7149.
19. **Khromykh, A. A., H. Meka, K. J. Guyatt, and E. G. Westaway.** 2001. Essential role of cyclization sequences in flavivirus RNA replication. J. Virol. 75:6719–6728.
20. **Khromykh, A. A., and E. G. Westaway.** 1996. RNA binding properties of core protein of the flavivirus Kunjin. Arch. Virol. 141:685–699.
21. **Kiermayr, S., R. M. Kofler, C. W. Mandl, P. Messner, and F. X. Heinz.** 2004. Isolation of capsid protein dimers from the tick-borne encephalitis flavivirus and in vitro assembly of capsid-like particles. J. Virol. 78:8078–8084.
22. **Kimura-Kuroda, J., M. Ichikawa, A. Ogata, K. Nagashima, and K. Yasui.** 1993. Specific tropism of Japanese encephalitis virus for developing neurons in primary rat brain culture. Arch. Virol. 130:477–484.
23. **Kofler, R. M., F. X. Heinz, and C. W. Mandl.** 2002. Capsid protein C of tick-borne encephalitis virus tolerates large internal deletions and is a favorable target for attenuation of virulence. J. Virol. 76:3534–3543.
24. **Lindenbach, B. D., and C. M. Rice.** 2001. *Flaviviridae*: the viruses and their replication, p. 991–1041. *In* D. M. Knipe, P. M. Howley, D. E. Griffin, R. A. Lamb, M. A. Martin, B. Roizman, and S. E. Straus (ed.). Fields virology, 4th ed., vol. 1. Lippincott Williams & Wilkins, Philadelphia, PA.
25. **Lo, M. K., M. Tilgner, K. A. Bernard, and P. Y. Shi.** 2003. Functional analysis of mosquito-borne flavivirus conserved sequence elements within 3′ untranslated region of West Nile virus by use of a reporting replicon that differentiates between viral translation and RNA replication. J. Virol. 77:10004–10014.
26. **Lobigs, M., and E. Lee.** 2004. Inefficient signalase cleavage promotes efficient nucleocapsid incorporation into budding flavivirus membranes. J. Virol. 78: 178–186.
27. **Ma, L., C. T. Jones, T. D. Groesch, R. J. Kuhn, and C. B. Post.** 2004. Solution structure of dengue virus capsid protein reveals another fold. Proc. Natl. Acad. Sci. USA 101:3414–3419.
28. **Makino, Y., M. Tadano, T. Anzai, S. P. Ma, S. Yasuda, and T. Fukunaga.** 1989. Detection of dengue 4 virus core protein in the nucleus. II. Antibody against dengue 4 core protein produced by a recombinant baculovirus reacts with the antigen in the nucleus. J. Gen. Virol. 70:1417–1425.
29. **Markoff, L., B. Falgout, and A. Chang.** 1997. A conserved internal hydrophobic domain mediates the stable membrane integration of the dengue virus capsid protein. Virology 233:105–117.
30. **Mathur, A., M. Bharadwaj, R. Kulshreshtha, S. Rawat, A. Jain, and U. C. Chaturvedi.** 1988. Immunopathological study of spleen during Japanese encephalitis virus infection in mice. Br. J. Exp. Pathol. 69:423–432.
31. **Matsuo, E., H. Tani, C. Lim, Y. Komoda, T. Okamoto, H. Miyamoto, K. Morilshi, S. Yagi, A. H. Patel, T. Miyamura, and Y. Matsuura.** 2006. Characterization of HCV-like particles produced in a human hepatoma cell line by a recombinant baculovirus. Biochem. Biophys. Res. Commun. 340:200–208.
32. **Mori, Y., T. Okabayashi, T. Yamashita, Z. Zhao, T. Wakita, K. Yasui, F. Hasebe, M. Tadano, E. Konishi, K. Morilshi, and Y. Matsuura.** 2005. Nuclear localization of Japanese encephalitis virus core protein enhances viral replication. J. Virol. 79:3448–3458.
33. **Nishinaka, T., Y. H. Fu, L. I. Chen, K. Yokoyama, and R. Chiu.** 1997. A unique cathepsin-like protease isolated from CV-1 cells is involved in rapid degradation of retinoblastoma susceptibility gene product, RB, and transcription factor SP1. Biochim. Biophys. Acta 1351:274–286.
34. **Oh, W., M. R. Yang, E. W. Lee, K. M. Park, S. Pyo, J. S. Yang, H. W. Lee, and J. Song.** 2006. Jab1 mediates cytoplasmic localization and degradation of West Nile virus capsid protein. J. Biol. Chem. 281:30166–30174.
35. **Oh, W. K., and J. Song.** 2006. Hsp70 functions as a negative regulator of West Nile virus capsid protein through direct interaction. Biochem. Biophys. Res. Commun. 347:994–1000.
36. **Okamoto, K., K. Morilshi, T. Miyamura, and Y. Matsuura.** 2004. Intramembrane proteolysis and endoplasmic reticulum retention of hepatitis C virus core protein. J. Virol. 78:6370–6380.
37. **Portaro, F. C., A. B. Santos, M. H. Cezari, M. A. Juliano, L. Juliano, and E. Carmona.** 2000. Probing the specificity of cysteine proteinases at subsites remote from the active site: analysis of P4, P3, P2′ and P3′ variations in extended substrates. Biochem. J. 347:123–129.
38. **Puzer, L., S. S. Cotrin, M. F. Alves, T. Egborge, M. S. Araujo, M. A. Juliano, L. Juliano, D. Bromme, and A. K. Carmona.** 2004. Comparative substrate specificity analysis of recombinant human cathepsin V and cathepsin L. Arch. Biochem. Biophys. 430:274–283.
39. **Reed, L. J., and H. Müench.** 1938. A simple method of estimationg fifty per cent endpoints. Am. J. Hyg. 27:493.
40. **Shaw, E., S. Mohanty, A. Colic, V. Stoka, and V. Turk.** 1993. The affinity-labelling of cathepsin S with peptidyl diazomethyl ketones. Comparison with the inhibition of cathepsin L and calpain. FEBS Lett. 334:340–342.
41. **Simmons, G., D. N. Gosalia, A. J. Rennekamp, J. D. Reeves, S. L. Diamond, and P. Bates.** 2005. Inhibitors of cathepsin L prevent severe acute respiratory syndrome coronavirus entry. Proc. Natl. Acad. Sci. USA 102:11876–11881.
42. **Solomon, T., H. Ni, D. W. Beasley, M. Ekkelenkamp, M. J. Cardosa, and A. D. Barrett.** 2003. Origin and evolution of Japanese encephalitis virus in southeast Asia. J. Virol. 77:3091–3098.
43. **Stocks, C. E., and M. Lobigs.** 1998. Signal peptidase cleavage at the flavivirus C-prM junction: dependence on the viral NS2B-3 protease for efficient processing requires determinants in C, the signal peptide, and prM. J. Virol. 72:2141–2149.
44. **Tadano, M., Y. Makino, T. Fukunaga, Y. Okuno, and K. Fukai.** 1989. Detection of dengue 4 virus core protein in the nucleus. I. A monoclonal antibody to dengue 4 virus reacts with the antigen in the nucleus and cytoplasm. J. Gen. Virol. 70:1409–1415.
45. **Tsai, T. F.** 2000. New initiatives for the control of Japanese encephalitis by vaccination: minutes of a WHO/CVI meeting, Bangkok, Thailand, 13–15 October 1998. Vaccine 18:1–25.
46. **Tsuda, Y., Y. Mori, T. Abe, T. Yamashita, T. Okamoto, T. Ichimura, K. Morlishi, and Y. Matsuura.** 2006. Nucleolar protein b23 interacts with Japanese encephalitis virus core protein and participates in viral replication. Microbiol. Immunol. 50:225–234.
47. **Wang, S. H., W. J. Syu, K. J. Huang, H. Y. Lei, C. W. Yao, C. C. King, and S. T. Hu.** 2002. Intracellular localization and determination of a nuclear localization signal of the core protein of dengue virus. J. Gen. Virol. 83: 3093–3102.
48. **Westaway, E. G., A. A. Khromykh, M. T. Kenney, J. M. Mackenzie, and M. K. Jones.** 1997. Proteins C and NS4B of the flavivirus Kunjin translocate independently into the nucleus. Virology 234:31–41.
49. **Yamshchikov, V. F., and R. W. Compans.** 1994. Processing of the intracellular form of the west Nile virus capsid protein by the viral NS2B-NS3 protease: an in vitro study. J. Virol. 68:5765–5771.
50. **Yang, K. D., W. T. Yeh, R. F. Chen, H. L. Chuon, H. P. Tsai, C. W. Yao, and M. F. Shaio.** 2004. A model to study neurotropism and persistency of Japanese encephalitis virus infection in human neuroblastoma cells and leukocytes. J. Gen. Virol. 85:635–642.
51. **Yasothornsrikul, S., D. Greenbaum, K. F. Medzihradszky, T. Toneff, R. Bundey, R. Miller, B. Schilling, I. Petermann, J. Dehnert, A. Logvinova, P. Goldsmith, J. M. Neveu, W. S. Lane, B. Gibson, T. Reinheckel, C. Peters, M. Bogyo, and V. Hook.** 2003. Cathepsin L in secretory vesicles functions as a prohormone-processing enzyme for production of the enkephalin peptide neurotransmitter. Proc. Natl. Acad. Sci. USA 100:9590–9595.
52. **You, S., B. Falgout, L. Markoff, and R. Padmanabhan.** 2001. In vitro RNA synthesis from exogenous dengue viral RNA templates requires long range interactions between 5′- and 3′-terminal regions that influence RNA structure. J. Biol. Chem. 276:15581–15591.
53. **You, S., and R. Padmanabhan.** 1999. A novel in vitro replication system for dengue virus. Initiation of RNA synthesis at the 3′-end of exogenous viral RNA templates requires 5′- and 3′-terminal complementary sequence motifs of the viral RNA. J. Biol. Chem. 274:33714–33722.
54. **Zhao, Z., T. Date, Y. Li, T. Kato, M. Miyamoto, K. Yasui, and T. Wakita.** 2005. Characterization of the E-138 (Glu/Lys) mutation in Japanese encephalitis virus by using a stable, full-length, infectious cDNA clone. J. Gen. Virol. 86:2209–2220.

Moriishi *et al*. 10.1073/pnas.0607312104.

Supporting Information

Files in this Data Supplement:

SI Figure 6
SI Figure 7
SI Methods and Materials

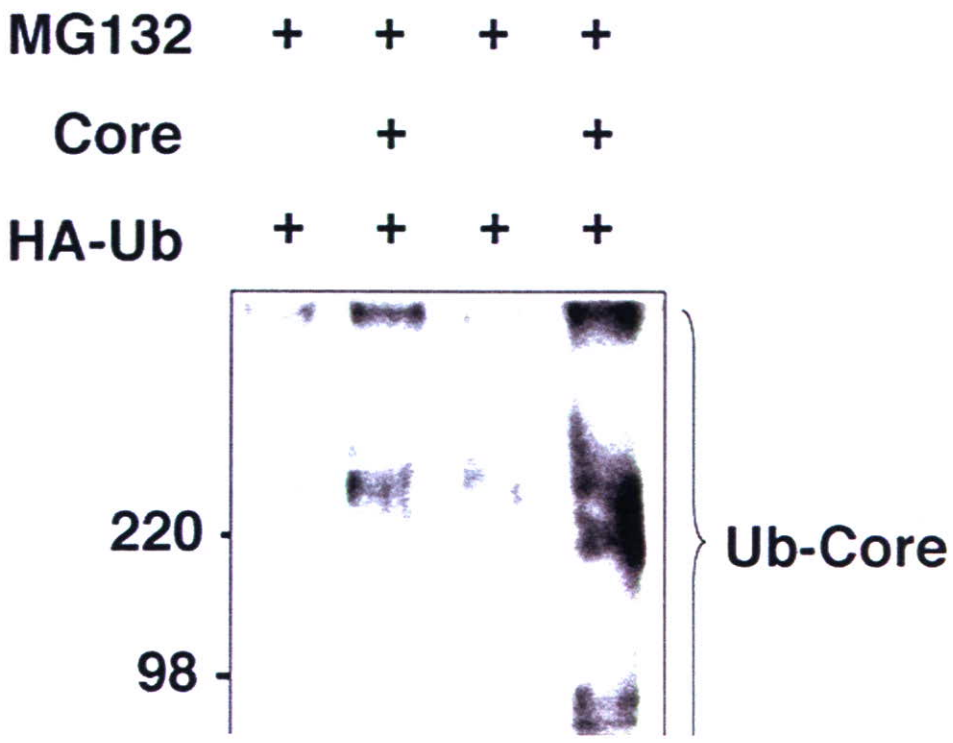

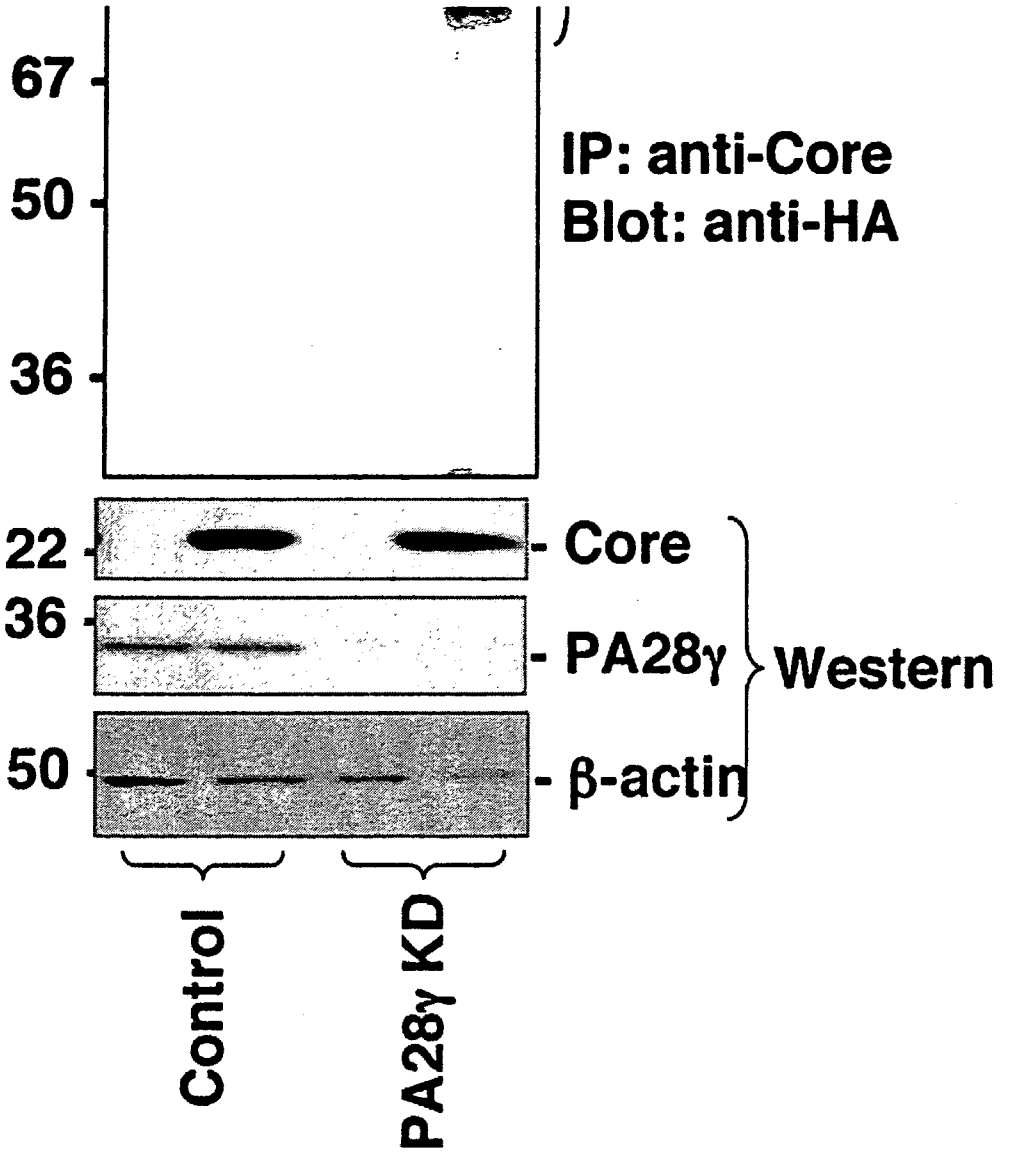

Fig. 6. Effect of PA28g knockdown on the ubiquitination of HCV core protein. HCV core protein was expressed with HA-tagged ubiquitin (HA-Ub) in the parental (Control) or PA28g-knockdown (PA28g KD) human hepatoma (FLC4) cells. The proteasome inhibitor MG132 was added to the culture supernatant at 24 h posttransfection to a final concentration of 10 mM. Cells were harvested at 36 h posttransfection, and cell lysates were subjected to immunoprecipitation (IP) with anti-core antibody and immunoblotting with anti-HA antibody (*Upper*). HCV core protein, PA28g, and b-actin in the cell lysate were detected by immunoblotting (*Lower*).

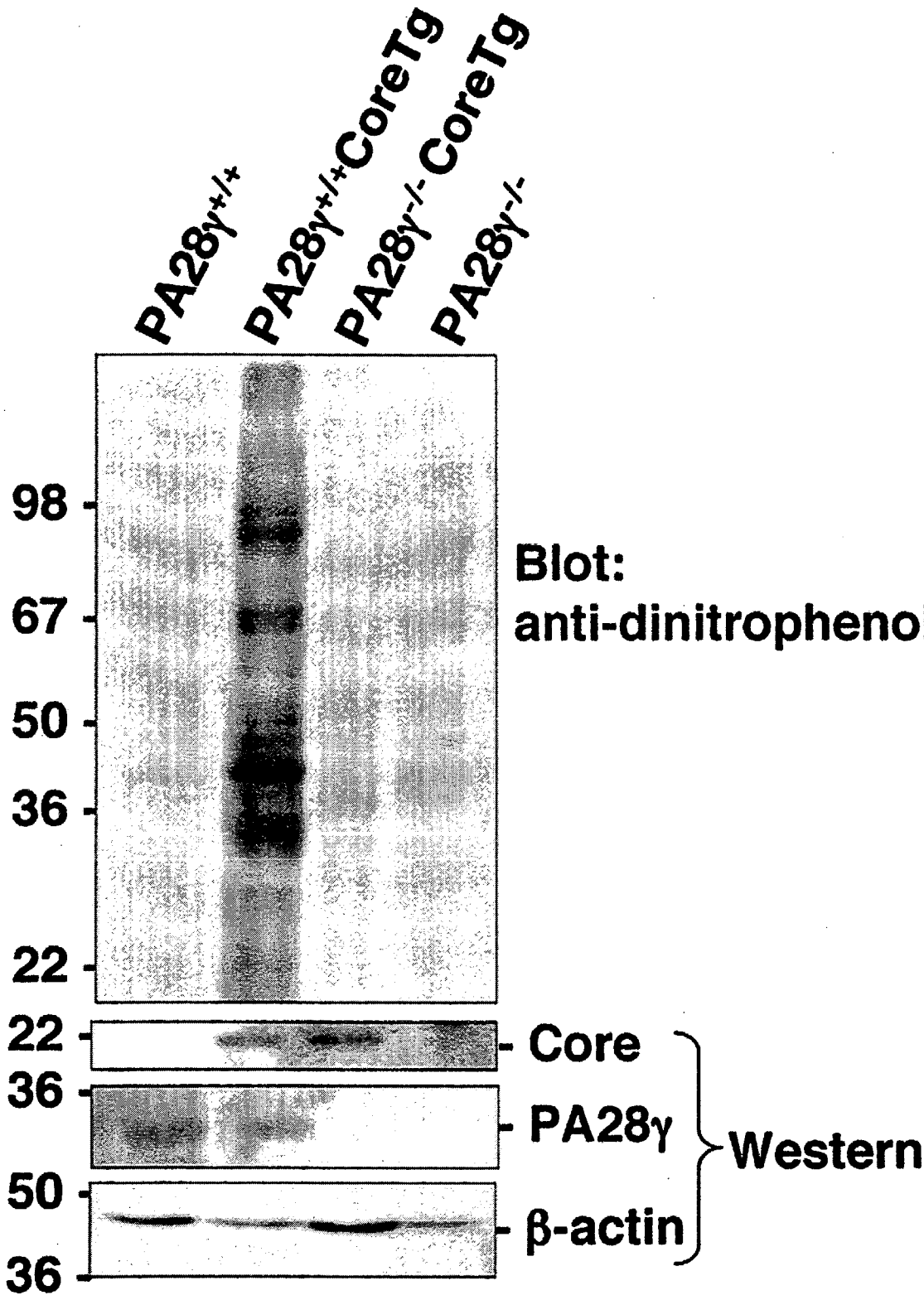

Fig. 7. Knockout of PA28g gene decreases the protein carbonylation induced by HCV core protein. Liver lysates were prepared from 6-month-old mice and subjected to OxyBlot assay. Each sample (20 mg of protein) was applied to a lane after the derivatization reaction (*Top*). HCV core protein, PA28g, and b-actin in the liver lysate were detected by immunoblotting (*Middle* and *Bottom*).

SI Methods and Materials

Histology and Immunohistochemistry. Formalin-fixed tissues were embedded in paraffin according to the standard procedures. Sections were stained with hematoxylin/eosin. To visualize lipids, frozen sections were stained with oil red O. For immunohistochemistry, sections of formalin-fixed tissues were treated with 3% (vol/vol) H_2O_2, washed twice with PBS, blocked with PBS containing 5% BSA, and incubated overnight with rabbit antibody to hepatitis C virus (HCV) core protein, followed by incubation with horseradish peroxidase-conjugated anti-rabbit IgG antibody (ICN, Aurora, OH) as a second antibody. Immunoreactive antigen was visualized with 3,3'-diaminobenzidine substrate. The percentage of the area occupied by oil red O-stained lipid droplets was calculated using Image-Pro software (MediaCybernetics, Silver Spring, MD). The area of the lipid droplets was examined in three different fields of every five randomly selected sections, and the areas were calculated by averaging 10 animals per genotype.

Real-Time PCR. RNA was prepared from the mouse livers with the use of TRIzol LS (Invitrogen, Carlsbad, CA). The first-strand cDNAs were synthesized with a first-strand cDNA synthesis kit (Amersham Pharmacia Biotech, Franklin Lakes, NJ). The amount of each cDNA was estimated by using Platinum SYBR Green qPCR super Mix UDG (Invitrogen) according to the manufacturer's protocol. The fluorescent signal was measured by using ABI prism 7000 (Applied Biosystems, Tokyo, Japan). The genes encoding mouse sterol regulatory element-binding proteins (SREBP)-1a, SREBP-1c, SREBP-2, stearoyl-CoA desaturase, acetyl-CoA carboxylase, fatty acid synthase, hydroxymethylglutaryl (HMG)-CoA synthase, HMG-CoA reductase, and hypoxanthine phosphoribosyltransferase were amplified with the primer pairs CACAGCGGTTTTGAACGAC and CTGGCTCCTCTTTGATCCCA, ACGGAGCCATGGATTGCACATTTG and TACATCTTTAAAGCAGCGGGTGCCGATGGT, ACCATTCTCCAGCAGTTCCGT and CCTCTCACAGTGACAGAAGGAGTT, TTCCCTCCTGCAAGCTCTAC and CGCAAGAAGGTGCTAACGAAC, GACAAACGAGTCTGGCTACT and TGATGAGTGACTGCCGAAAC, CTCCAAGACTGACTCGGCTACT and AGCTGGGAGCACATCTCGAA, GGTTGGAGTGTTCTCTTACGG and CTCTGACCAGATACCACGTTC, TATGCCCATCCCTGTTGGAG and CACGTGGAGTTTCTGTAGACGA, and CCAGCAAGCTTGCAACCTTAACCA and GTAATGATCAGTCAACGGGGGAC, respectively. The sense and antisense primers were located in different exons to avoid false-positive amplification from contaminated genomic DNA. Each PCR product was confirmed as a single band of the correct size by agarose gel electrophoresis (data not shown).

Detection of Proteins Modified by Reactive Oxygen Species. Carbonyl groups in proteins were detected by using an OxyBlot kit (Chemicon International, Temecula, CA) according to the manufacturer's instructions. The carbonyl groups in the side

chains of amino acid residues included in the protein are a hallmark of the oxidation status of proteins, and they are reacted with 2,4-dinitophenylhydrazine, resulting in the derivatization to 2,4-dinitrophenylhydrazone. The derivatized proteins are subjected to SDS/PAGE and Western blotting using the antibody to dinitrophenyl moiety.